U.PORTO

FEUP FACULDADE DE ENGENHARIA UNIVERSIDADE DO PORTO

INTEGRATED MASTER IN ENVIRONMENTAL ENGINEERING 2019/2020

CHARACTERIZATION AND OPTIMIZATION OF AN ELECTROCHEMICAL SYSTEM FOR CARBON DIOXIDE REMOVAL

FRANCISCO MIGUEL AZEVEDO LIMA

Dissertation submitted for the degree of

MASTER ON ENVIRONMENTAL ENGINEERING

President of the jury:
Cidália Botelho, Professora Auxiliar do Departamento de Engenharia Química da Faculdade de Engenharia da Universidade do Porto

---

Supervisor at FEUP:
Alexandra Pinto, Professora Associada do Departamento de Engenharia Química da Faculdade de Engenharia da Universidade do Porto

---

Supervisor at Wetsus:
Qingdian Shu, Researcher at Wetsus, European Centre of Excellence for Sustainable Water Technology

---

July 2020

“Climate change is no longer some far-off problem; it is happening here; it is happening now.”

Barack Obama

Acknowledgements

The following work was only made possible with the contributions from a lot of people throughout the years. I would like to thank them all on this section for their help, in many ways, through the period of writing my thesis but also throughout all my academic life.

First, my supervisor at Wetsus, Qingdian Shu, who was instrumental in the writing of this thesis and in sharing his knowledge during my internship. A word to all the people at Wetsus, from the lab technicians to my coworkers, that made working at Wetsus a special experience, especially all the friends who shared with me those memories in Leeuwarden.

This work was only possible due to the skills I developed during the rest of my course, so I also want to thank my teachers that taught me so much in these years, especially my supervisor professor Alexandra Pinto, for her help, and professor Cidália Botelho, who was able to help me with my Erasmus application. A word to all my classmates, that also helped me by sharing their knowledge.

Finally, I also want to thank my mother and father, who I owe everything to, and the rest of my family and friends, who have been a huge support all these years. Thank you all, I am very grateful.

Abstract

Climate change is a challenge mankind is facing in present times. Rising Carbon Dioxide levels in the atmosphere have led to increasing temperatures around the globe. This rising temperature brings problems for wildlife and populations around the world, by many ways such as rising sea levels and agricultural deficiencies.

Because of this it is important to reduce the amount of Carbon Dioxide in the atmosphere. This greenhouse gas has a long life in the atmosphere, so reducing emissions while essential is not enough to stop climate change. Direct Air Capture shows promising results in removing the Carbon Dioxide already present in the atmosphere. Through techniques of absorption or adsorption, it is possible to capture Carbon Dioxide to these solvents and afterwards through a regeneration method, usually a pressure or a temperature swing, release the Carbon Dioxide.

Alkaline hydroxides show promise for Direct Air Capture, however current methods to regenerate the sorbent require temperatures up to 900^{o}C. In this work we propose an alternative regeneration method by way of a pH swing, that does not require such high temperatures and should be able to reduce the energy consumption in this step of the process.

When sodium hydroxide reacts with Carbon Dioxide it forms sodium carbonate. However, if the pH of this solution is lowered, it will form bicarbonate and afterwards gaseous Carbon Dioxide. This pH swing is achieved with the use of an electrochemical system that will move protons into this solution, removing the sodium ions that can also react with hydroxide to regenerate the capture solution, releasing gaseous Carbon Dioxide.

To make the system as efficient as possible it was necessary to characterize it, so we defined three parameters that are decisive to the system. The Load Ratio, that relates the number of ions that we introduce in the system with the number of ions that the current we apply can move from the solution. The Current Density that is applied, that is the current chosen divided by the area of the membrane in use. The initial sodium concentration, that defines the number of ions we introduce in the system.

With these parameters being defined several experiments were made, with the system being optimized with a Load Ratio of 0.8, a Current Density of 50 A/m^2 and a sodium concentration of 1M. The best result obtained was 360 kJ/mol, which when compared with results observed in literature, shows that this system can be competitive and can be an alternative for Carbon Dioxide regeneration methods in current Direct Air Capture facilities.

LIST OF CONTENTS

FIGURES INDEX

TABLES INDEX

1 INTRODUCTION

Our planet's atmosphere has remained unchanged in the last 500 million years (Hart, 1978), being mainly composed of nitrogen and oxygen, but also other trace gases, which allow for the possibility of human life (Karl & Trenberth, 2003).

However, changes have been observed mainly in the concentration of Carbon Dioxide (CO_2). The concentration of this gas in the atmosphere has been increasing since the Industrial Revolution, surpassing the highest historical CO_2 levels in 1950 as seen in Figure 1 and continuing to rise to this day. Measurements based on air extracted from ice cores allows to determine that in 1750 CO_2 had a concentration in the atmosphere of 278 parts per million (ppm) Hartmann et al. (2013), while in November 2019, the concentration of CO_2 in the atmosphere was 410 ppm, measured by the Global Monitoring Lab of the National Oceanic and Atmospheric administration. This change in concentration shows a growth of 47.4%, between the years of 1750, that can be considered the start of the anthropogenic era when the industrial revolution began (Ruddiman, 2003), and current times.

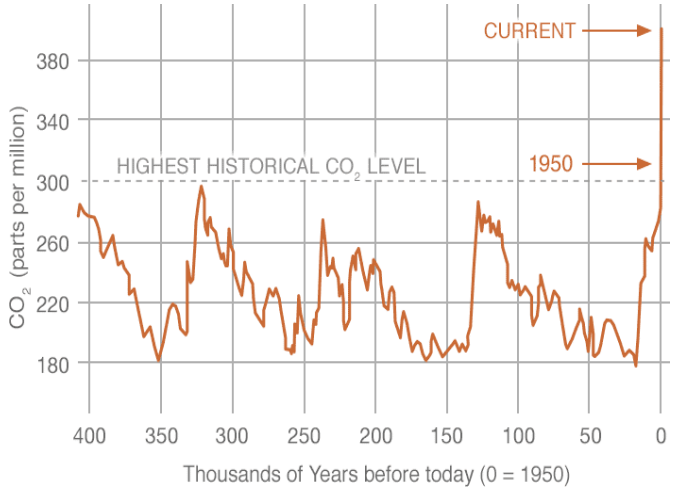

FIGURE 1 - CO2 CONCENTRATION OVER THE LAST 400 THOUSAND YEARS (SOURCE: CLIMATE.NASA.GOV)

The increase in CO_2 can be correlated to anthropogenic emissions (Ciais et al., 2014). The larger demands of energy and the use of fossil fuels associated to it has led directly to a higher concentration of CO_2, which has led to a higher Global Mean Surface Temperature due to the heat-trapping nature of the CO_2 gas. Records have shown that over the period between 1880, when the recording of this data starts, and 2012, that represents the current times, Global Mean Surface Temperature increased at about 0.85^{o}C, and as observable in Figure 2, this increase follows the one seen in CO_2 concentration (Hartmann et al., 2013).

A higher Global Mean Surface Temperature will lead to worldwide problems. One of these is the rise in mean sea levels, which will cause problems such as erosion and inundations. It can also cause a higher number of events such as heat waves and glacial retreats have been observed and may lead to slope instabilities and movements of mass. Also changes in heavy precipitations will most likely affect landslides in certain regions (Field, Barros, Stocker, & Dahe, 2012).

The increase in Global Mean Surface Temperature will also provoke changes in the hydrological cycle, that can alter the balance between food supply and demand in many parts of the world, with regions like South Asia and Africa being particularly vulnerable to these kind of changes due to their limited resources, large populations and dependence on agriculture (Aggarwal & Singh, 2010).

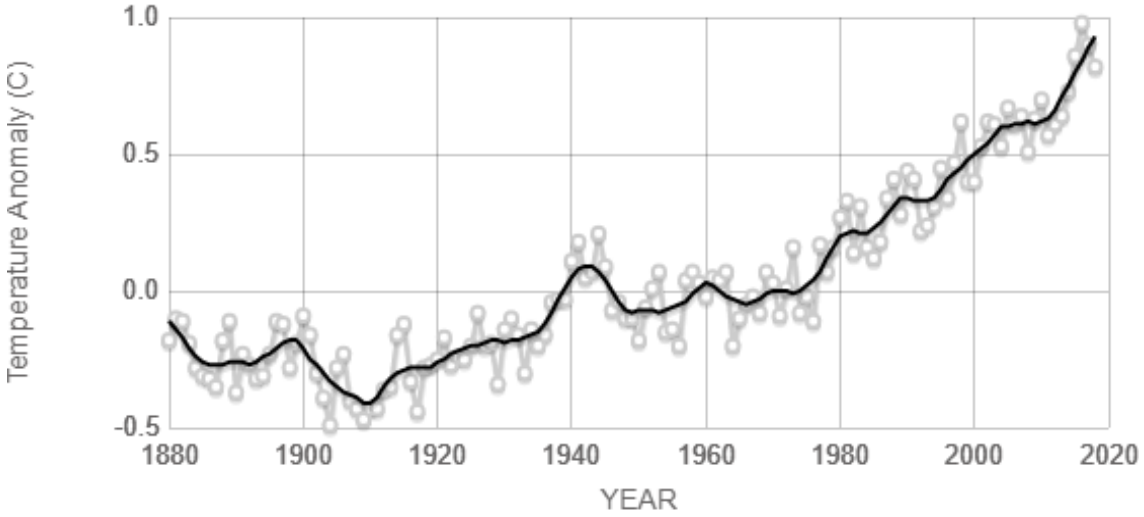

FIGURE 2 - EVOLUTION OF GLOBAL MEAN SURFACE TEMPERATURE (SOURCE: CLIMATE.NASA.GOV)

To limit the increasing temperatures and the risks associated to it, the United Nations signed the Paris Agreement in which the UN countries agreed to cut greenhouse emissions to hold the increase in the global average temperature to well below 2^{o}C above pre-industrial levels and pursuing efforts to limit the temperature increase to 1.5^{o}C above pre-industrial levels. By 2015 the temperature had already increased by 0.87^{o}C compared to pre-industrial times and at this pace the 1.5^{o}C barrier would be surpassed around 2040 (Allen et al., 2018), so in order to comply with the Paris Agreement, the United Nations countries need to make bigger efforts to reduce Greenhouse Gases (GHG) emissions.

Technological developments have been made throughout history to capture post-combustion CO_2. Carbon Capture Use and Storage (CCUS) refer to a multitude of technologies that can limit GHG emissions, and can store, or utilize, the captured CO_2. However, although a reduction in GHG emissions is vital to lessen the impacts of climate change, the Intergovernmental Panel on Climate Change (IPCC) has reported that even an immediate reduction to zero emissions would barely be enough to achieve the goal of limiting temperature increase below 1.5^{o}C below pre-industrial levels (Allen et al., 2018). Moreover, the GHG emissions realistically cannot be reduced immediately to zero.

These considerations along with the fact that CO_2 is a long-lived greenhouse gas that can impact the Global Mean Surface Temperature for several centuries (Matthews & Caldeira, 2008), reveal the importance of Negative Emission Technologies. The planet can function as a Negative Emission Technology by itself, due to the ocean being a carbon sinkhole, and the plants photosynthesis, these natural techniques however are too slow to be relied upon for the removal of CO_2 from the atmosphere (Archer & Brovkin, 2008), hence the need for anthropogenic Carbon Dioxide Removal.

This is how Direct Air Capture (DAC) appears as a solution for this problem as this type of technology can effectively remove atmospheric CO_2 (Sanz-Perez, Murdock, Didas, & Jones, 2016). Even though DAC is still in the first stages of development, it already shows favorable results, which indicates that this technology will be a very important tool in the fight against global warming (Fasihi, Efimova, & Breyer, 2019).

In this work, we propose an electrochemical system for DAC that is easy to operate and consume less energy comparing to other technologies. We have done the primary characterization of system in terms of energy consumption and sorbent recovery efficiency under different operational conditions.

2 STATE OF THE ART

2.1 Historical Background

The first developments of CO_2 capture technology were done in the 1930s in cryogenic air separation plants (House et al., 2011). Further advancements occurred with the need to recycle air in closed systems such as submarines and space stations. The latter started by using lithium hydroxide cannisters for CO_2 removal. Afterwards, to allow for longer missions in space, regenerable sorbents were introduced. Zeolite beds were used to adsorb the CO_2 and then they were regenerated using a pressure-swing followed by a temperature-swing.(Winton et al., 2016)

As stated previously CCUS technologies have existed for the past several decades being used in many projects. Although the technologies described in this type of sector are mainly applied to point source emissions, as they are not able to fully remove GHG emissions from the atmosphere (Leeson, Mac Dowell, Shah, Petit, & Fennell, 2017), the theoretical background and the developments over the decades can offer us a theoretical background to separate CO_2 from a gas mixture on DAC systems.

2.2 Carbon Capture Technologies

CCUS is divided into several steps: capture, transport, use and storage. The first step is the one we will focus on as it is the step devoted to in this research.

The main two capture technologies used in CCUS are absorption and adsorption, each presenting advantages and drawbacks, and are described as the following:

2.2.1 Absorption

In absorption processes CO_2 molecules are dissolved into the bulk phase of a solvent, as seen in Figure 3. Absorption processes typically consist of an absorber and a stripper, in which the absorbent is regenerated usually by a temperature swing. The gas containing CO_2 enters a packed bed absorber and contacts counter-currently with the absorbent. After the absorption process the CO_2-rich absorbent, having removed it from the gas, is directed into a stripper for the regeneration process. The CO_2 released from the stripper can be compressed for future storage, while the regenerated absorbent can be utilized in the absorber again for another CO_2 absorption cycle (Yu, Huang, & Tan, 2012). A schematic of the conventional absorption-regeneration process is represented in Figure 4.

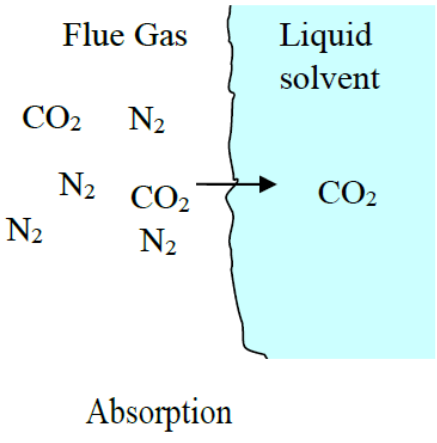

FIGURE 3 – CO_2 ABSORPTION MECHANISM (SOURCE: NATIONAL PETROLEUM COUNCIL, USA)

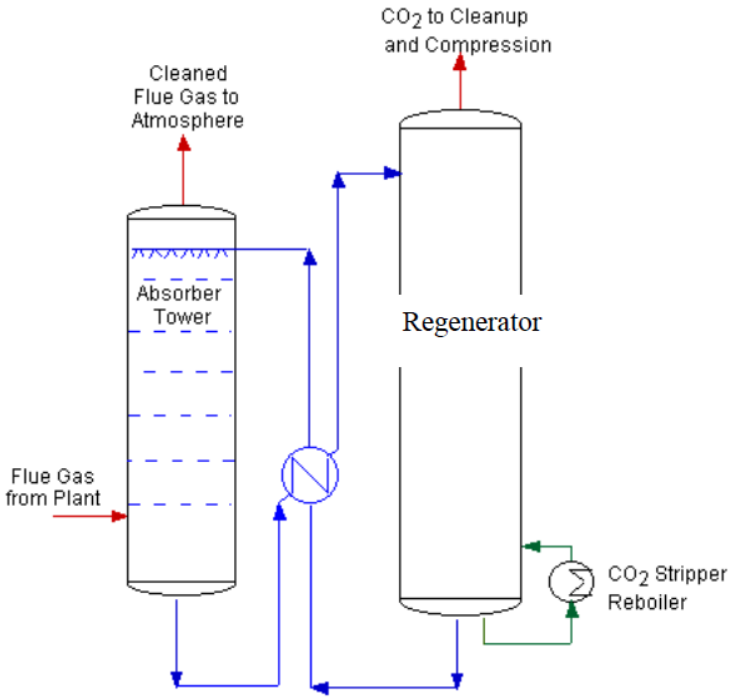

FIGURE 4 – SCHEME OF A CONVENTIONAL ABSORPTION-REGENERATION PROCESS (SOURCE: NATIONAL PETROLEUM COUNCIL, USA)

Typical absorbents used are aqueous alkaline hydroxide solutions, specifically sodium hydroxide, potassium hydroxide and calcium hydroxide. These solutions can absorb CO_2, however they also present strong binding to CO_2 which requires large energy demands in the regeneration step (Broehm, Strefler, & Bauer, 2015). The reaction between the CO_2 and the alkaline hydroxide solutions forms alkaline carbonate species.

Potassium hydroxide despite showing the most favorable results for CO_2 capture among alkalines (Hayashi et al., 1998), is not as commonly employed as sodium hydroxide or calcium hydroxide due to its higher costs (Goeppert, Czaun, Prakash, & Olah, 2012). Sodium hydroxide presents advantages over calcium hydroxide as it allows for higher concentrations to be used, which will result in more CO_2 being captured (Broehm et al., 2015).

The sodium carbonate that results from the reaction between sodium hydroxide and CO_2 is usually regenerated by reacting it with Calcium Hydroxide, resulting in the regeneration of the sodium hydroxide and a calcium carbonate precipitate. This precipitate can be removed with the use of a kiln, where the CO_2 is released. However, this solution requires very high temperatures, of around 900^{o}C, in the regeneration step and may lead to the buildup of solids that will affect the equipment (Baciocchi, Storti, & Mazzotti, 2006).

CO_2 absorption can also be done by use of amine sorbents, the most common one being monoethanolamine. When reacting with the CO_2 these amines initially form a carbamate, that afterwards, via hydrolysis, forms bicarbonate (MacDowell et al., 2010).

The regeneration step for amine sorbents is done through thermal regeneration in a stripper, at lower temperatures, around 130^{o}C, than the ones used to regenerate the alkaline hydroxides. However, using this type of sorbent can lead to other problems due to amine degradation. Specifically, if the oxygen content present in the flue gas is higher than 5% the amine can be exposed to oxidative degradation (Yu et al., 2012).

2.2.2 Adsorption

In adsorption processes the CO_2 molecules stick to the surface of another material due to weak Van der Waals forces (physisorption) or strong covalent bonding forces (chemisorption). A representation of a CO_2 adsorption process with a solid sorbent can be seen in Figure 5. The materials can absorb molecules due to their porous structure and can have selectivity, that will absorb a certain type of molecule, like CO_2 in this instance, more than other molecules (Oschatz & Antonietti, 2018). Selectivity is determined by the affinity the sorbent material has to a certain species over another. In the case of carbon capture, it is the ratio between the affinity of the sorbent material to CO_2 with the affinity of the sorbent material to N_2, as nitrogen is usually a component of flue gas streams (Radosz, Hu, Krutkramelis, & Shen, 2008).

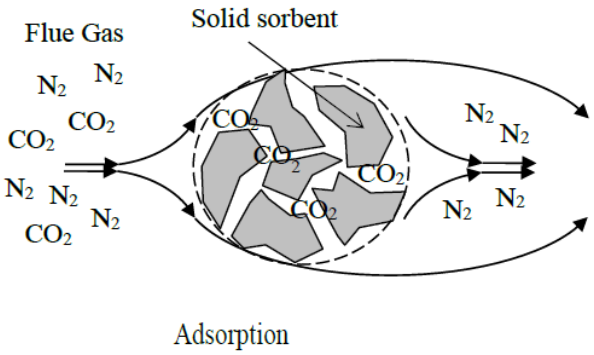

FIGURE 5 - CO2 ADSORPTION MECHANISM BY USE OF A SOLID SORBENT (SOURCE: NATIONAL PETROLEUM COUNCIL, USA)

Materials for CO_2 adsorption are selected if they present a high CO_2/N_2 selectivity. But this property of the material can also be influenced by other parameters such as pressure (Radosz et al., 2008) or the surface area and pore structure of the adsorbent (Yu et al., 2012).

Usually packed beds or fluidized beds are used for this process. The captured gas flows through the bed where the CO_2 is adsorbed by the sorbent and once saturation is reached the flow gas is stopped to allow for the separation of the CO_2 from the sorbent. This separation step is done through a pressure-swing or temperature-swing process. This process is represented in Figure 6.

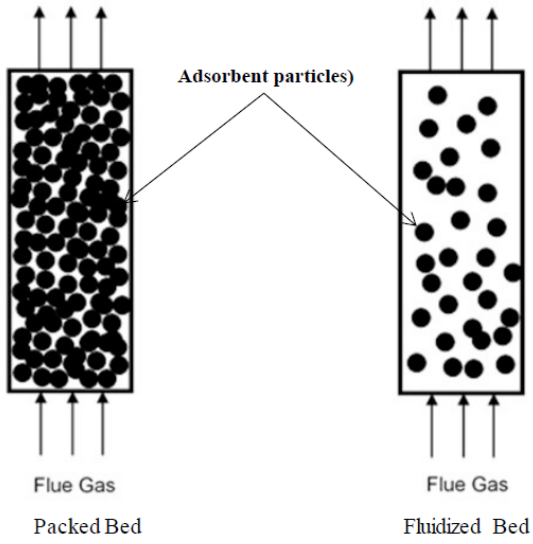

FIGURE 6 - SCHEME OF AN ADSORPTION PROCESS WITH A PACKED BED OR A FLUIDIZED BED (SOURCE: NATIONAL PETROLEUM COUNCIL, USA)

Common materials used as adsorbents are activated carbon and zeolites. Zeolites can present narrow pore size distribution that allows for a high CO_2 selectivity and also have high adsorption capacities at ambient pressure with high thermal stability, reaching 600^oC (Oschatz & Antonietti, 2018). Typically, zeolites show a hydrophilic character, so in the presence of moisture in the gas stream, their adsorption capacity declines considerably (Yu et al., 2012). Furthermore, zeolites may adsorb CO_2 strongly, creating a more difficult regeneration process as there would need to be more energy to separate the CO_2 from the sorbent (Cheung & Hedin, 2014)

Activated carbon have advantages over zeolites as it is a cheaper material, and does not present a hydrophilic character, which makes this material more adequate if the gas stream possesses moisture. Moreover, the regeneration step for this material has been done using nearly half of the energy required to regenerate zeolites (Plaza, García, Rubiera, Pis, & Pevida, 2010). However, compared to zeolites, activated carbon shows a weaker affinity to CO_2, because of this it has a lower CO_2/N_2 selectivity (Oschatz & Antonietti, 2018).

Pressure-swing regeneration is mostly used for sorbents that capture CO_2 through physisorption, as is the case of activated carbon and zeolites. Usually, the adsorption step is done at a higher than atmospheric pressure while the regeneration step is done at atmospheric pressure (Yu et al., 2012). Temperature-swing is used for sorbents that capture CO_2 through chemisorption like amine-functionalized resins. These sorbents have lower heat capacity compared to liquid solvents, which leads to a lower heat requirement in the regeneration step (Alesi Jr & Kitchin, 2012). In this process the adsorption is done at temperatures between 30^oC and 40^oC, while the regeneration is done at temperatures between 120^oC and 135^oC, with this higher temperature being provided by hot air or steam (Yu et al., 2012).

2.3 Direct Air Capture

The process of capturing CO_2 directly from the atmosphere was first introduced in 1999 by Klaus Lackner (Lackner, Ziock, & Grimes, 1999), where the feasibility of this technology was first discussed. Since then, many studies related to this technology have helped developing it and have shown that DAC plants can be set up in any place and can be used to address point source emissions as well as the ones from mobile emitters (Sanz-Perez et al., 2016).

In a DAC process, contactors are used to bring the ambient air in contact with the sorbent (Keith, Holmes, St. Angelo, & Heidel, 2018), while facilitating airflow through the module and maximizing the contact area between the sorbents and the CO_2 molecules (Fasihi et al., 2019).

The capture process itself is the first step and the main technologies used are, as described above, absorption with liquid solvents, and adsorption with solid sorbents. The three most established companies in this sector use these technologies. Carbon Engineering is established in Canada and operates a pilot plant that is able to capture one ton of CO_2 per day using a liquid solvent (Fasihi et al., 2019). This plant operates as demonstrated in the Figure 7. Air contacts a Potassium Hydroxide (KOH) solution, producing Potassium Carbonate (K_2CO_3), which afterwards reacts with Calcium Hydroxide (CaOH). This reaction results in the recovery of the capture solution of KOH and of the precipitation of Calcium Carbonate ($CaCO_3$). The solid $CaCO_3$ is fed into a calciner, where it is heated up to a temperature of around 900^oC, where CO_2 is extracted and the resulting Calcium Oxide (CaO) is fed into a slaker where the CaOH solution is recovered, this process results in an energy consumption of 8.81 GJ/ton of CO_2 when using natural gas as fuel (Keith et al., 2018).

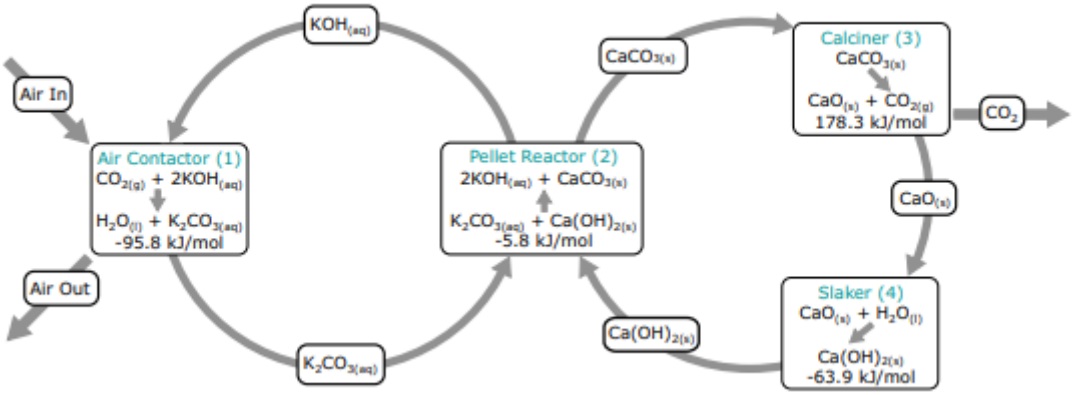

FIGURE 7 - CARBON ENGINEERING PROCESS DESCRIPTION (SOURCE: KEITH, HOLMES ET AL, 2018)

The other two main companies in DAC technologies operate with solid sorbents. Climeworks operates in Switzerland and has built the first commercial-scale DAC plant. Their technology uses a filter made of porous granulates modified with amines. When the gas stream contacts the filters, the CO_2 molecules bind to the amines. Once the filter is saturated with CO_2, it is heated to 100°C. At this temperature, the bond is broken, and the CO_2 is released from the filter and can be collected, while the filter is regenerated. The regeneration process used by Climeworks uses between 1500 and 2000 kwh/ ton of CO_2 (Vogel, 2017). This amounts to between 5.4 and 7.2 GJ/ton of CO_2.

Global Thermostat operates in the United States and their system uses an amino-polymer adsorbent to capture the CO_2. The regeneration step occurs using temperatures between 85-95°C along with the use of saturated steam at sub-atmospheric pressures as a sweep gas (Fasihi et al., 2019). Global Thermostat energy consumption is reported to be between 1170 and 1410 kwh/ton of CO_2 (Ping, Sakwa-Novak, & Eisenberger, 2018), which amounts to between 4.2 and 5.1 GJ/ton of CO_2.

As discussed previously the choice of sorbent is essential to improve the efficiency of the DAC process. The use of amine sorbents for atmospheric CO_2 capture may be limited, as the oxygen content present in the atmosphere is well above the 5% mark and the degradation that occurs in amine sorbents in these conditions may be harmful for human health and the environment (MacDowell et al., 2010).

Physical adsorption may also be limited as this type of sorbents present low selectivity for CO_2 (Broehm et al., 2015) and due to the low concentration of this gas in the atmosphere this proves to be a challenge for the use of solid sorbents in DAC, being more suited for CCUS projects, revealing the need for identification for a more suitable material for adsorption.

3 THEORETICAL BACKGROUND

As described before, liquid solvents are more commonly used in DAC pilot plants. However, the regeneration step of the process is normally done using very high temperatures, around 900°C (Keith et al., 2018). The focus of this work lies on using an alternative method for this regeneration step, by using an electrochemical system that does not require such high temperatures.

When the Carbon Dioxide reacts with the alkaline hydroxide, in use for the capture step, it results on an alkaline carbonate and bicarbonate solution. The use of an electrochemical system allows to apply a current that can transfer protons lowering the post-capture solution pH. As it can be seen on Figure 8, as the pH reaches a more acidic value, the carbonate present in the solution reacts into bicarbonate and afterwards into Carbonic Acid (H_2CO_3), which is a weak acid that can turn into CO_2 (g) (Nagasawa, Yamasaki, Iizuka, Kumagai, & Yanagisawa, 2009). Equations 1 to 4 describe the evolution of the reaction from Carbonate to gaseous CO_2.

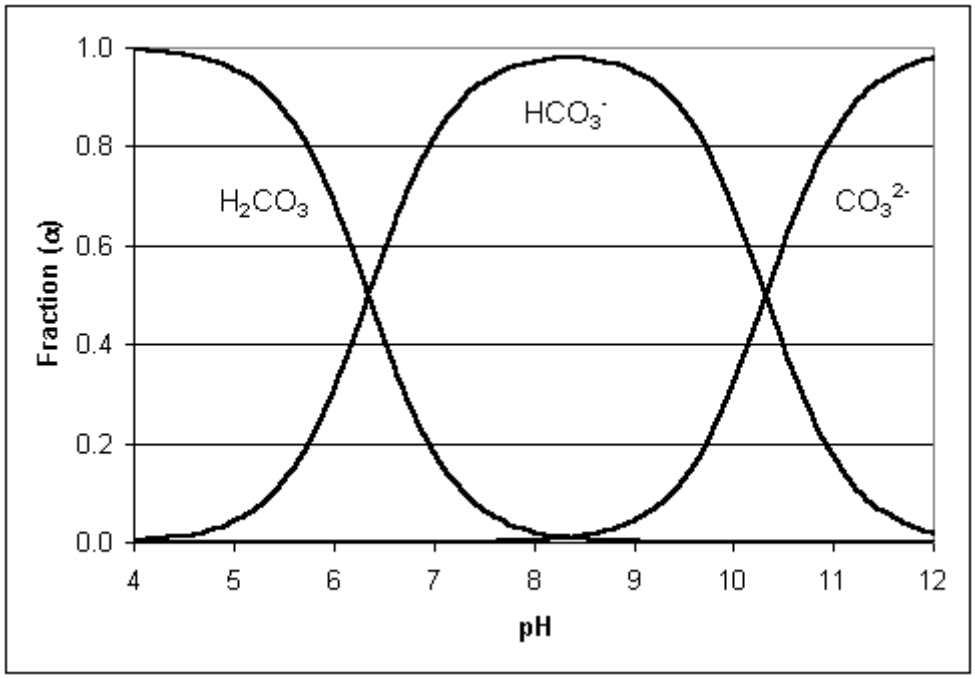

FIGURE 8 - FRACTION OF CARBONIC ACID, CARBONATE AND BICARBONATE IN RELATION WITH PH (SOURCE: BOSNICH, 2011)

$$CO_3^{2-} + H^+ \Leftrightarrow HCO_3^- \ (1)$$

$$HCO_3^- + H^+ \Leftrightarrow H_2CO_3 \ (2)$$

$$H_2CO_3 \Leftrightarrow H_2O + CO_2 \ (aq) \ (3)$$

$$CO_2 \ (aq) \Leftrightarrow CO_2 \ (g) \ (4)$$

Electrochemical systems are comprised by two electrodes, separated by an electrolyte, and connected via an external electronic conductor. There is a flow of ions from one electrode to the other, while through the external conductor electrons flow to maintain the electro neutrality of the system (Newman & Thomas-Alyea, 2012).

In the electrodes the electrochemical reactions occur. These reactions are redox reactions with the distinction that they do not happen at the same place. So, in the positively charged electrode, the anode, an oxidation reaction will occur, while in the negatively charged electrode, the cathode, a reduction

reaction will ensue. The reactions and the movement of charged particles are obtained by applying a current in the system (Newman & Thomas-Alyea, 2012).

To introduce the post-capture solution to the system, there needs to be a separate compartment other than the anode and the cathode. This compartment is separated by Ion-Exchange Membranes (IEM) that only allow the passage of certain types of particles, so when the current is applied, a specific ionic species can be moved to a different compartment, while other, undesired species, are blocked from moving. Ion-exchange membranes can be Anion Exchange Membranes (AEM), that only allow anions to go through, or Cation Exchange Membranes (CEM), that only allow cations to go through.

To achieve this solution an electrochemical system based on the one used for ammonia recovery will be used (Kuntke et al., 2017). The system in use comprises of three compartments, that are the anode, acidifying and cathode compartments, separated by two CEMs. A scheme of the system used is represented by Figure 9.

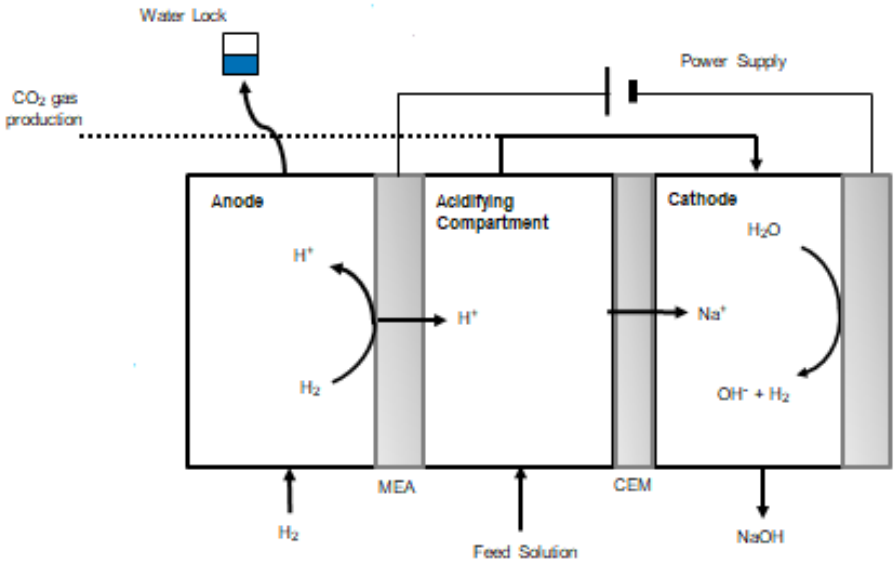

FIGURE 9 - SCHEME OF THE ELECTROCHEMICAL SYSTEM USED FOR CO_2 DESORPTION

In the anode, H^+ ions are generated, by the oxidation of hydrogen. Hydrogen is produced in an electrolyzer and is afterwards fed to the anode. The anode is a Membrane Exchange Assembly (MEA) that is formed by a Gas Diffusion Electrode (GED) and a CEM. The GDE is a porous carbon electrode that makes the gas distribute evenly in the electrode so when the current is applied H_2 is oxidized.

In the acidifying compartment CO_2 is desorbed. A solution is fed to this compartment that mimics the composition resulting from the reaction between Sodium Hydroxide (NaOH) and CO_2. The composition of the solution is determined using the partial pressure of carbon dioxide in the gas mixture and the molar mass of Sodium present in the capture solution, the Sodium Hydroxide.

The protons formed at the anode flow through the CEM, replacing the Na^+ present in the solution, and are able to lower the pH in the stream allowing for the bicarbonate and carbonate present in the stream to generate CO_2 as shown in Equations 1-4. In the cathode sodium hydroxide is formed. Water is reduced generating OH^- and hydrogen. The hydroxide ions react with the Na^+ that pass through the CEM that separates the acidifying compartment and the cathode. This reaction allows the recovery of the sorbent that can be used for more capture of atmospheric CO_2. In this study, to minimize the energy consumption of the system, we characterize and optimize the system in order to find the best set of parameters for the most energy efficient removal of CO_2.

4 MATERIALS AND METHODS

The setup for this project is described in Figure 10. The system used comprised three compartments, anode, acidifying and cathode compartments. The anode was a Membrane Exchange Assembly (MEA), composed by an integrated Gas Diffusion Electrode (GDE) coated with a 10cm X 10 cm of Platinum – Vulcan (carbon) catalyst (0.5 mg Pt cm^{-2}) and a 15cm X 15 cm Nafion N117 Cation Exchange Membrane (CEM) from FuelCellsEtc (Texas,USA). A catalyst was also present for the oxidation to occur at a faster rate and a lower potential. The GDE side faced the anode compartment, while the CEM was facing the acidifying compartment.

The protons were transported through the MEA to the acidifying compartment. Once in this compartment the protons lowered the pH. The low pH was able to, as described previously, react the carbonate and bicarbonate in the feeding solution into gaseous carbon dioxide. The resulting solution was pumped out at 150 ml/min and was passed through a membrane contactor to remove the gas that was afterwards measured in a flow rate measurer.

The acidifying compartment, situated between anode and cathode compartments, was created by using a polymeric (nitril) spacer (500 µm, Sefar,Switzerland).

The acidifying compartment was separated from the anode by the MEA, and from the cathode by a Nafion N117 CEM (15 cm X 15 cm) FuelCellsEtc (Texas,USA).

The cathode was a Ru/Ir coated titanium mesh electrode (9.8 cm x 9.8 cm, Magneto Special Anodes BV, the Netherlands).

The housing of the anode and the cathode was made from poly(methylmethacrylate) (PMMA (21 cm X 21 cm X 2.5 cm)), with a machined flow field (10 cm X 10 cm X 0.2 cm).

Silicone Rubber Gaskets were used to create a water/gastight seal in the electrochemical systems.

An electrolyzer, operating at constant current, was used to supply H_2 to the anode. The electrolyzer used a solution of 0.025 M of H_2SO_4 and comprised an anode a cathode and a CEM between the two electrodes. In the anode water was oxidized generating oxygen gas and protons. The protons flowed to the cathode through the CEM and reacted with the hydroxide produced in the cathode. The reduction of water in this system also produced hydrogen which was then redirected to the anode in the main cell depicted in Figure 10 to produce the protons.

Both the electrolyzer and the system operated at constant current (CC) provided by a power supply (ES 030-5, Delta Elektronika BV, Zierikzee, The Netherlands).

Three Masterflex peristaltic pumps (Masterflex L/S, Metrohm Applikon BV, Schiedam, The Netherlands) were used to supply new solution to the system, recirculate the solution in the system and to extract the alkaline hydroxide produced at the cathode. While another of these pumps was used for the electrolyzer.

A membrane contactor (type MM 1.7 x 8.75, 3M, USA) was used to separate the gaseous CO_2 from the solution that goes through the acidifying compartment. The gas stream was afterwards dehumidified by a Nafion Tubing (TUB-0003, CO2Meter.com, USA) and measured with a mass flow meter (EL-Flow Prestige, Bronkhorst High-Tech B.V., Ruurl, The Netherlands).

To measure the potential difference in the anode, the cathode and across the CEM placed between the acidifying compartment and the cathode, reference electrodes were placed before the acidifying compartment inlet and cathode inlet. The reference electrodes were connected to a high impedance

preamplifier (Ext-Ins Technologies, Leeuwarden, The Netherlands) and to a multimeter (Fluke 8846 A, Fluke Europe B.V, Eindhoven, The Netherlands).

Conductivity sensors (Memosens CLS82D, Endress+Hauser BV, The Netherlands) and pH sensors (Orbisint CPS11D, Endress+Hauser BV, The Netherlands) were used to measure these parameters. These sensors were connected to a Liquiline CM444 transmitter (Endress+Hauser BV, Naarden, The Netherlands).

To record the values for pH, conductivity, anode potential and cathode potential an Ecograph T RSG 35(Endress + Hauser BV) was used.

Two recirculation loops were added to the acidifying and cathode compartments, respectively. The overflow from acidifying recirculation was redirected to the cathode recirculation. The recirculation flow rate was fixed at 150 mL/min.

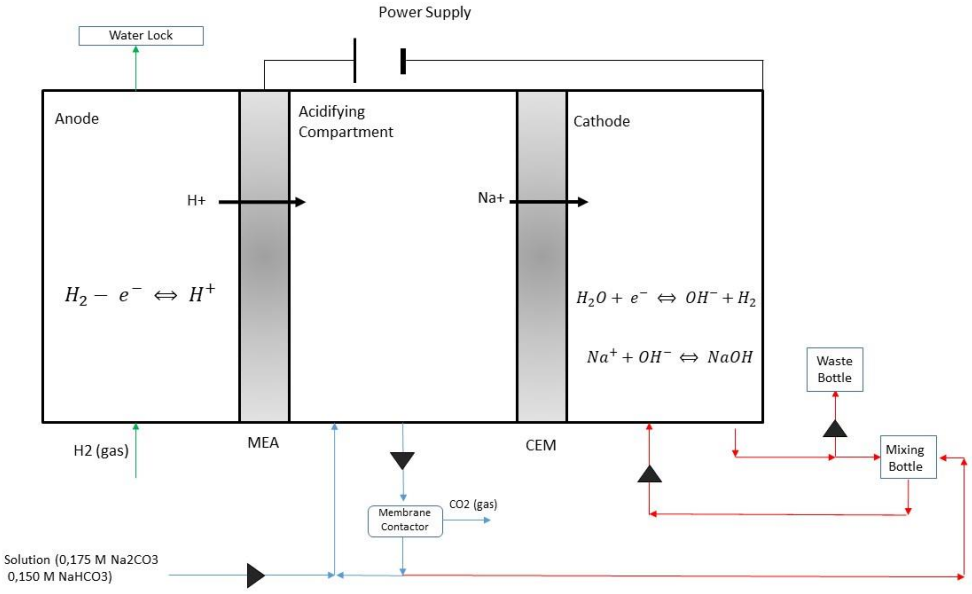

FIGURE 10 - RESEARCH SETUP SCHEME

4.1 Research Questions

To be able to remove CO_2 from the feeding solution we need to be able to lower the pH in the acidifying compartment. With this system this is achieved by moving the protons generated in the anode to the acidifying compartment. To move these protons an electrical current is applied. The current applied is able to transport the protons through the CEM into the acidifying compartment, where they replace the sodium ions. These sodium ions then have to move from the acidifying to the cathode compartment through the CEM (Willauer, DiMascio, Hardy, Lewis, & Williams, 2011).

So, in theory a high enough current would be able to move all the ions away from the acidifying compartment. This would lead to a lower conductivity in this compartment, which would also, in accordance with Ohm's Law, lead to a higher voltage being applied. This would mean that the energy consumption would be very high, as stated previously.

The current density applied determines the rate of ion transport, but also the quantity of carbonate and bicarbonate that enters the system have implications on the performance of the system. To relate these different parameters Load Ratio is used. Load Ratio describes the ratio between applied current density and the sodium load expressed as current density (Kuntke et al., 2017). This means that the Load Ratio

describes the ratio of Na^+ in the influent that can be transported with the current applied. The transport of Na^+ determines the transport of H^+, which will affect the pH change in the acidifying compartment. So, the Load Ratio can indicate the CO_2 production performance of the system.

Load Ratio can be calculated with the use of Equation 5:

$$L_{Na^+} = \frac{i_A}{(C_{Na^+} * Q_{feed} * \frac{1}{A} * F)} \quad (5)$$

With i_A being the current density in A/m^2, C_{Na^+} being the concentration of sodium ions in the solution in mol/L, Q_{feed} is the flow rate of the solution being pumped into the system in L/s, A is the membrane area in m^2 and F is the Faraday Constant in C/mol.

The area considered is the membrane area, with a value of 100 cm^2, as we are using a 10x10 cm membrane. The Faraday Constant has a value of 96485 C/mol. The concentration of carbonate and bicarbonate obtained if the capture solution had a concentration of 0.5N of NaOH in equilibrium with 0.04% of CO_2 in the air are 0.175M and 0.15M, respectively. These concentrations allow for an initial concentration of Na^+ of 0.5M to be used for the Load Ratio calculation.

With these values always being constant we can alter the current we apply on the system and the flow rate we use to get the load ratio we want.

With a Load Ratio lower than 1 there is more Na^+ ions that the current can transport. A Load Ratio higher than 1 means that the Na^+ ions in the solution are in deficit to the current applied (Rodriguez Arredondo, Kuntke, Ter Heijne, Hamelers, & Buisman, 2017).

If the Load Ratio is 1 that means, in theory that the current we are applying is able to transport all the Na^+ ions to the cathode.

So, a Load Ratio higher than 1 would not be very efficient because we would be supplying current in excess to the particles we want to transport. This excess is not needed so it would be a waste of energy.

A Load Ratio of 1 can also be detrimental to the system because moving all the Na^+ ions away from the acidifying compartment would lower the conductivity there, which would lead to an increase in the voltage, which would lead to a higher energy consumption.

However, as stated previously, the Load Ratio also determines how much CO_2 we are producing in the system. So, a low Load Ratio may not be able to produce enough CO_2 for it to be energetically feasible as the energy consumption is measured by mol of CO_2 produced.

The main research question is then, to define at what Load Ratio can the system be more energy efficient. To find this ideal Load Ratio several test will be done at different flow rates and current densities, to varying Load Ratio values, to make sure that the system is retrieving the most CO_2 at the lowest energy consumption.

After finding this ideal Load Ratio other tests can be done to find the ideal concentration of the feeding solution. So, another question to be asked is at what concentration of the feeding solution the system will be more efficient.

For the Ammonia Recovery, the equilibrium voltage, anode overpotential and transport potential losses over the CEM between feed and cathode compartments were the main contributors to overall potential losses (Kuntke et al., 2017). Overpotential increases with the current density applied, so the last question to be asked is if at the ideal Load Ratio could we apply low current densities, and therefore low flow rates,

to decrease the overpotential, and as a result decrease the energy consumption and increase the efficiency of the system.

4.2 Figures of Merit

Energy consumption is the main obstacle keeping DAC from becoming a viable solution to reduce atmospheric CO_2 concentrations. To determine how this system compares to other DAC projects it is imperative to calculate its energy demand. Furthermore, the amount of capture solution recovered in the system is an important parameter to analyze how the system preforms.

The energy consumption, in kJ/mol, is calculated through the use of Equation 6:

$$E = \frac{V \times A \times 60}{\frac{CO_2 Production}{1000}} \quad (6)$$

V, in Volts, is the Voltage when the system is at steady state. A, in Amps, is the current applied to the system. CO_2 Production, in mol/min, is obtained through Equation 7:

$$CO_2 Production = \frac{GasProduction^* \times P}{T \times R \times 10^{-6}} \quad (7)$$

Gas Production, is the gas production recorded through the use of mass flow meters in mLn/min. P is the pressure in the system, which is the atmospheric pressure in Pa. T represents temperature, in K, which is constant at 298.15 K. And R is the ideal gas constant in J/mol.K.

The capture solution recovery percentage is determined by Equation 8:

$$NaOH_{Recovery} = \frac{[NaOH_{Cathode}]}{[Na_{initial}]} \quad (8)$$

The concentration of Sodium Hydroxide at the cathode is obtained using OLI software, after measuring the pH in this compartment at steady state. The initial Sodium concentration is fixed at the start of each experiment.

5 RESULTS AND DISCUSSION

5.1 Experiments with Different Load Ratio

The first set of experiments, described in Table 1, was done by changing the Load Ratio conditions. The Current Density was set at 150 A/m^2 and the Na^+ concentration at 0.5M. Using a range between 0.2 and 1.2 for Load Ratio with the rest of the parameters fixed implied a flow rate change. Flow rates varied between 9.33 mL/min and 1.55 mL/min, with the former corresponding to the lowest Load Ratio value and the latter to the highest.

TABLE 1 - SET OF CONDITIONS FOR EXPERIMENTS WITH DIFFERENT LOAD RATIOS

Flow Rate (mL/min)	Na Concentration (mol/L)	Current Density (A/m^2)	Load Ratio
9.33	0.5	150	0.20
4.66	0.5	150	0.40
3.11	0.5	150	0.60
2.67	0.5	150	0.70
2.33	0.5	150	0.80
2.07	0.5	150	0.90
1.86	0.5	150	1.00
1.55	0.5	150	1.20

As seen in Figure 8 the lower the pH value is, the less carbonate and bicarbonate are present and therefore more gaseous CO_2 can be released. However, we will also have less ionic species present in the solution resulting in a lower conductivity value, that results in a higher voltage applied to the system and consequentially a higher energy consumption. So, to minimize the energy consumption of the system we need to characterize and optimize the system in order to find the best set of parameters for the most energy efficient removal of CO_2.

With this set of experiments, it is possible to see that the pH values go through visible changes with increasing Load Ratio. The pH in the Acidifying Compartment gets significantly lower, while the pH in the Cathode Compartment for the lowest Load Ratio values remains very close to the initial value of 9.5. For the remaining Load Ratio values, it increases steadily to values ranging between 12.16 and 13.48. These changes can be seen graphically in Figure 11.

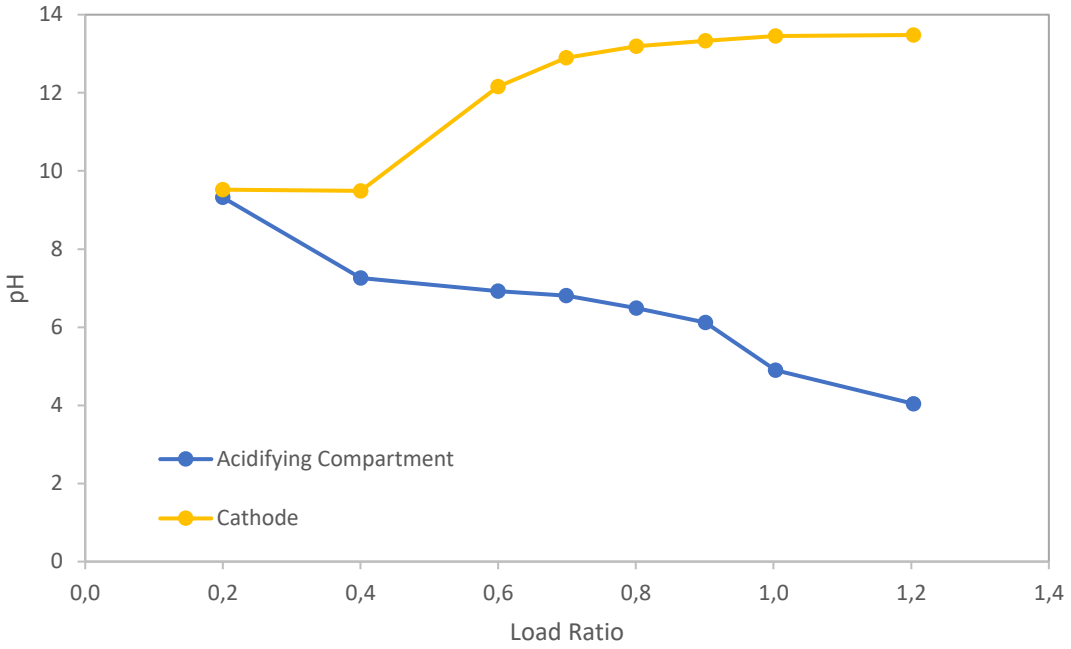

FIGURE 11 - VARIATION OF PH IN ACIDIFYING AND CATHODE COMPARTMENTS WITH INCREASING LOAD RATIO

With a fixed applied Current Density, the rate of protons being introduced to the Acidifying Compartment is constant for all the experiments. However, with higher influent flow rates, it means that the concentration of protons in the compartment is lower. As we increase the Load Ratio, we are increasing the concentration of protons present in the solution we are introducing in the system, so the pH is lowered in this compartment.

In the Cathode Compartment, the opposite is observable. With increasing Load Ratio values there is an increase in the pH. This is due to more OH^- being available. This is a strong base that strongly influences the pH of the solution, making it more basic. A higher Load Ratio means that more carbon is desorbed, so less carbon species are able to react with the hydroxide forming carbonate that does not lower the pH as much.

As expected for Load Ratio values under 1, the CO_2 production rate increases with the Load Ratio, as it can be seen in Figure 12. With the lowest Load Ratio value, no gas production was observed. This was expected as the Acidifying Compartment pH for this experiment at steady state is not low enough to desorb CO_2, so the current applied was not enough to change the pH and make the bicarbonate and carbonate react to form gaseous CO_2, when using such a high flow rate.

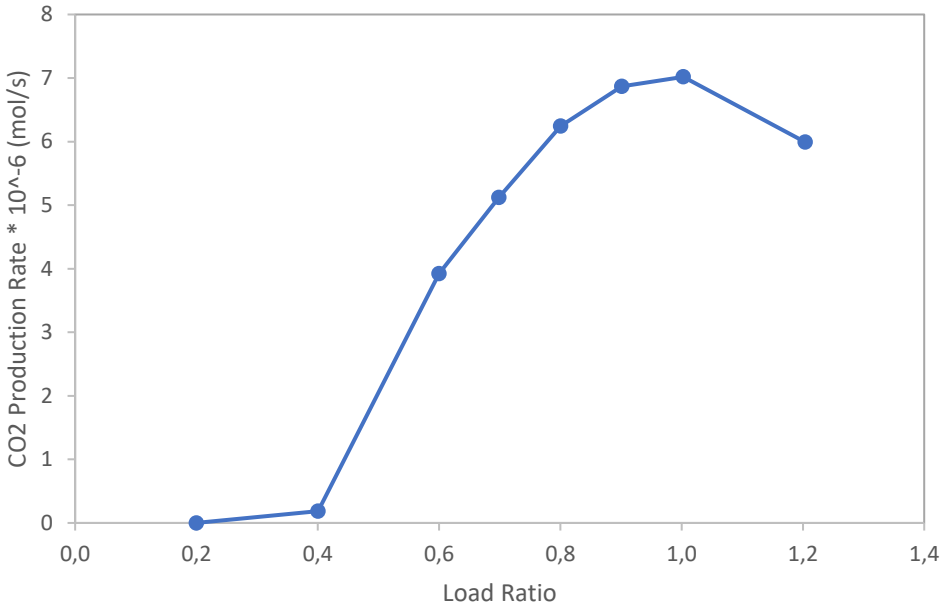

FIGURE 12 - VARIATION OF CO2 PRODUCTION RATE WITH INCREASING LOAD RATIO

The gas production rate reaches a peak at a Load Ratio of 1. The Load Ratio 1.2 experiment showed even lower gas production rate than the 0.8 Load Ratio experiment. In the Load Ratio 1.2 experiment the Acidifying Compartment pH is low enough that most of the carbon species present are in the form of $H_2CO_3^*$. So, in this case, the carbon removal efficiency is mostly limited by the CO_2 partial pressure in the gas phase of the membrane contactor, which is constant at 1atm. This means that the CO_2 production is limited by the amount of carbon that we supply to the system and not by the pH in the Acidifying Compartment. The amount of carbon that is supplied to the system decreases, since the flow rate is lower as we increase the Load Ratio, so less total carbon is available to be desorbed at a higher Load Ratio. At Load Ratio 1 the balance between the pH that is low enough to desorb most of the carbon species in the solution and the lower flow rate, and subsequent lower total carbon supplied, allows for the best CO_2 production rate out of all the experiments made in this set.

The Conductivity is correlated to the pH, so it experiences similar changes, as it can be observed in Figure 13. In the Acidifying Compartment, it steadily decreases with Increasing Load Ratio. This is because with higher Load Ratio values we are moving more Na^+ ions to the Cathode Compartment, meaning that there are less Na^+ ions in the Acidifying Compartment. With higher Load Ratio values, we are also producing more gaseous CO_2, so we have less Carbonate and Bicarbonate ions. As we have less ions present in the compartment, the conductivity decreases.

In the Cathode Compartment, it increases significatively with the increase in Load Ratio. This is also due to the movement of more Na^+ ions to this compartment, but especially due to more OH^- being present, which are highly conductive, and as such, contribute greatly to the increase in conductivity in the Cathode. The higher Load Ratio also means that there is more carbon being desorbed, so there is less carbon that can react with the hydroxide to form carbonate. Hydroxide has a higher molar conductivity than carbonate, so the increase in Load Ratio leads to a noticeable increase in conductivity in the Cathode Compartment.

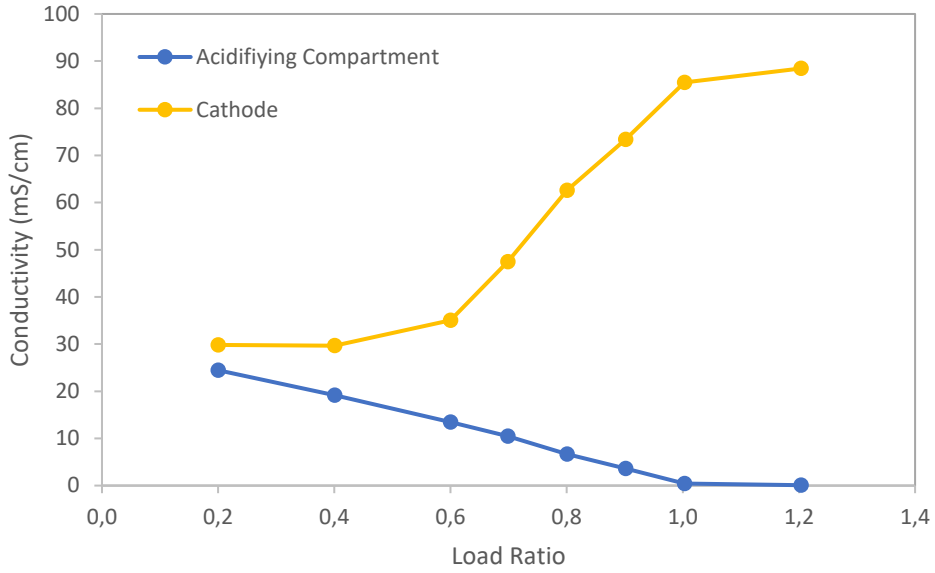

FIGURE 13 - VARIATION OF CONDUCTIVITY IN ACIDIFYING AND CATHODE COMPARTMENTS WITH INCREASING LOAD RATIO

Despite showing the highest CO_2 production rate, the experiment with a value of Load Ratio of 1, has the highest energy consumption out of the experiments with Load Ratio ranging from 0.6 to 1, with a value of 1550 kJ/mol. The lowest energy consumption was achieved at 0.8 Load Ratio, with a value of 485 kJ/mol, as it can be observed in Figure 14, while recovering 45% of NaOH. For this graph, the points for the experiments with Load Ratio 0.2, 0.4 and 1.2 were not considered as these experiments resulted in the highest energy consumptions. For the experiments with Load Ratio 0.2 and 0.4 the gas production was too little, while for the Load Ratio 1.2 experiment, the internal resistance was too high. So, for an easier reading of the graph only the five points represented were considered.

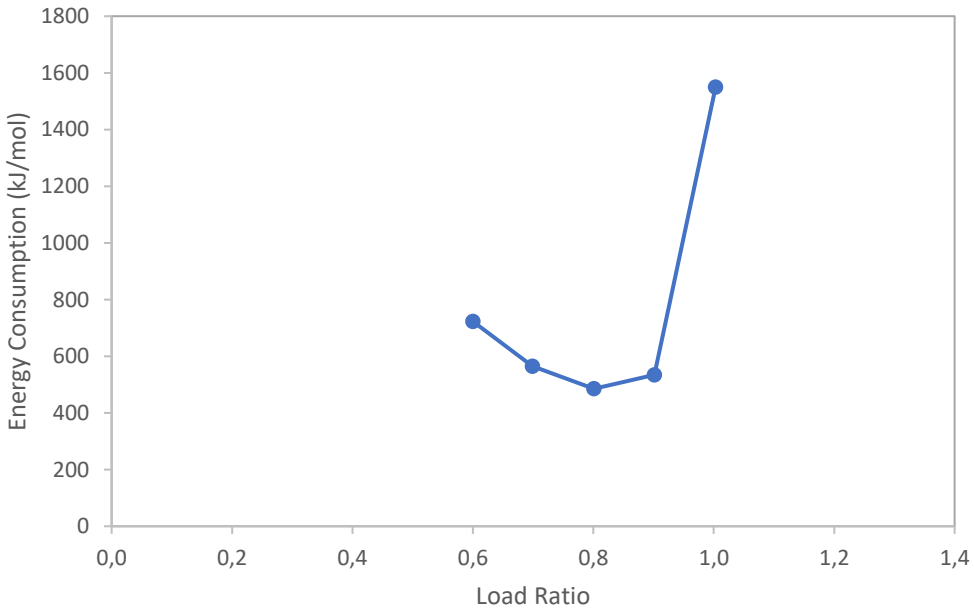

FIGURE 14 - VARIATION OF ENERGY CONSUMPTION WITH INCREASING LOAD RATIO

This shows that applying a current to the system that moves the entirety of Na^+ ions present in the solution is not optimal. When moving all the ions from the solution we are decreasing substantially the conductivity as it can be seen in Figure 13. With a lower conductivity, the resistance will increase and with that the voltage as well, this leads to an increase in energy consumption, and the higher CO_2 production rate is not enough to offset the increases in energy that this Load Ratio leads to. The best result was with a Load Ratio of 0.8, which was the Load Ratio defined for the next sequence of experiments.

5.2 Experiments with Different Current Densities

After finding the ideal Load Ratio, the next set of experiments, described in Table 2, were made with differing current densities to find at what value will the system operate more efficiently. Fixing the Na^+ concentration and the Load Ratio, it is possible to determine the flow rates for the different current densities that were applied. Current densities between 25 and 300 A/m^2 were used.

TABLE 2 - SET OF CONDITIONS FOR EXPERIMENTS WITH DIFFERENT CURRENT DENSITIES

Flow Rate (mL/min)	Na Concentration (mol/L)	Current Density (A/m^2)	Load Ratio
0.39	0.5	25	0.80
0.78	0.5	50	0.80
1.55	0.5	100	0.80
2.33	0.5	150	0.80
4.66	0.5	300	0.80

As seen in figure 15, the current density does not have an influence in the pH. This is due to the fixed Load Ratio we are using; with the same Load Ratio we have the same ratio of Na^+ being replaced by H^+ ions in the Acidifying Compartment. The Load Ratio also defines the ratio of OH^- production rate to influent flow rate, so for the Cathode Compartment the pH is also constant. For increasing current densities no relevant changes were observed. This allows us to see that the Load Ratio is the parameter that has more impact on the systems pH evolution, and the values at its steady state.

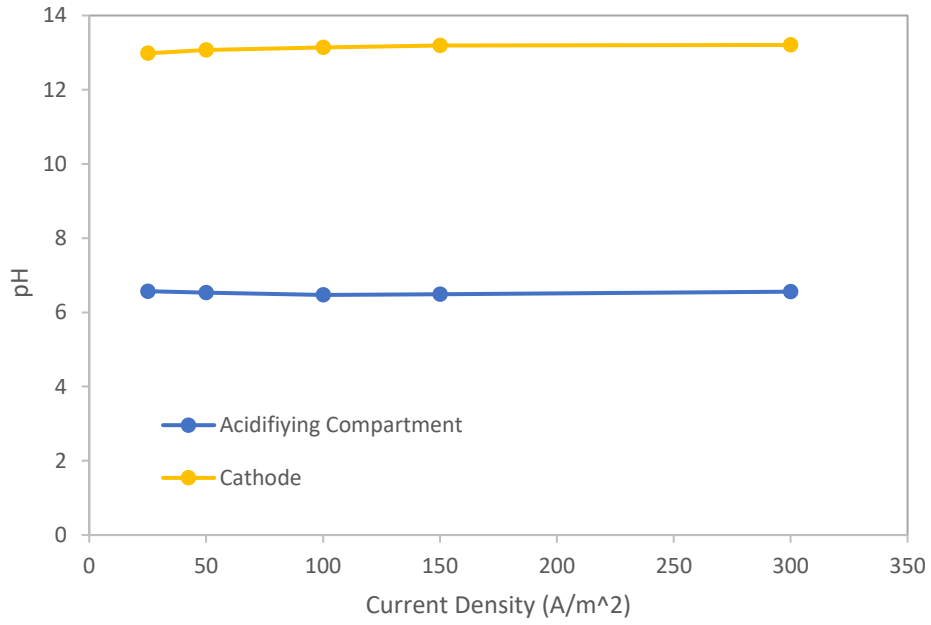

FIGURE 15 - VARIATION OF PH IN ACIDIFYING AND CATHODE COMPARTMENTS WITH INCREASING CURRENT DENSITY

Current applied is related to the number of particles moved per second. So, a higher current will move more protons into the acidifying compartment per second and remove more Na^+ ions per seconds. This means that we can expect the CO_2 production rate to increase with the current density. The results obtained comply with the theory, as we observe exactly this in Figure 16. The highest current density shows the highest CO_2 production per second, with the increase being almost linear.

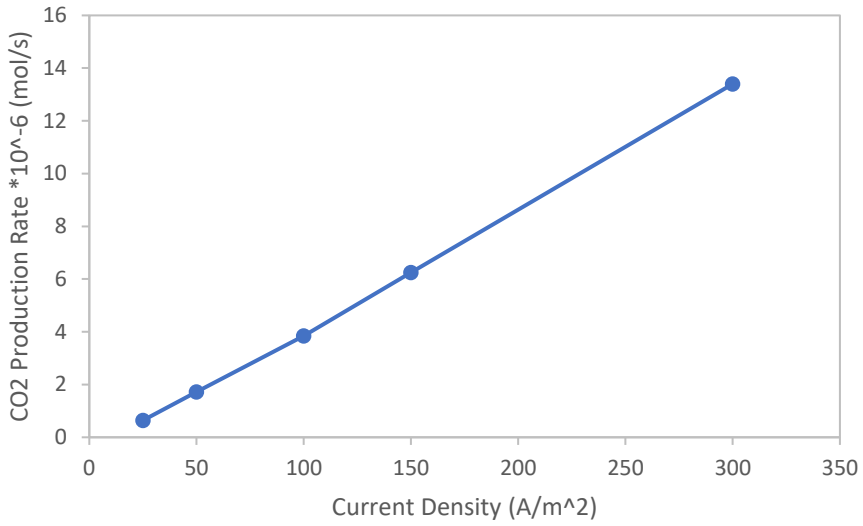

FIGURE 16 - VARIATION OF CO2 PRODUCTION RATE WITH INCREASING CURRENT DENSITY

As the pH is mostly constant for each current density applied, the conductivity also presents similar values throughout the different experiments. However, a notable difference is seen as the conductivity in the Cathode Compartment increases with the current density, as it can be observed in Figure 17. This increase is mainly due to the non-ideal separation of CO_2 after the Acidifying Compartment. With lower current density a higher percentage of CO_2 remained in the solution and recombined with the OH^- ions produced at the cathode. This results in the production of carbonate ions that have lower molar conductivity than hydroxide.

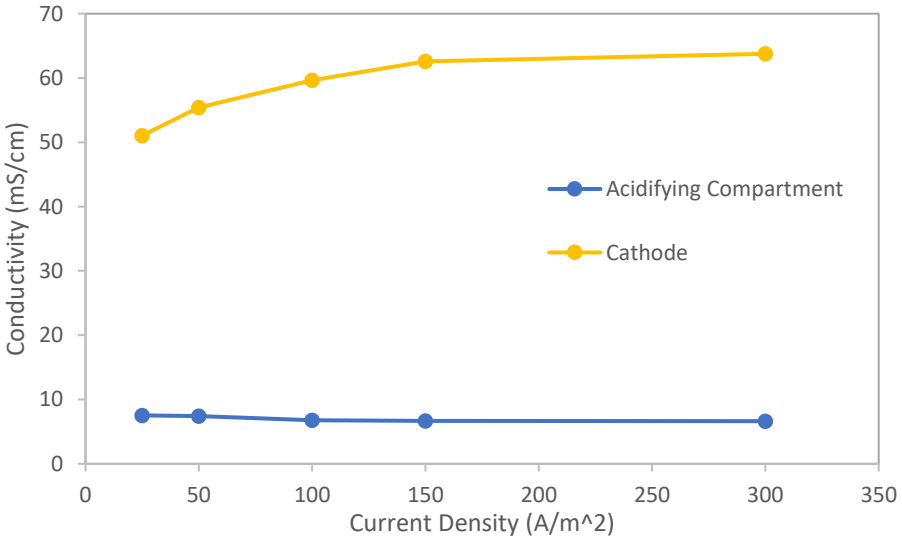

FIGURE 17 - VARIATION OF CONDUCTIVITY IN ACIDIFYING AND CATHODE COMPARTMENTS WITH INCREASING CURRENT DENSITY

Figure 18 shows the results of Energy Consumption in kJ/mol for this set of experiments. The highest current density produces the most CO_2 per second, however, that only means that the reaction occurs faster. So, despite that, it also has the highest energy consumption out of the experiments made in this set, as this calculation is done per mol. This was expected as the increase in current density leads to a higher overpotential, which itself leads to this increase in energy consumption.

However, it was observed that the best result was obtained not at the lowest current density of 25 A/m^2 but for the one immediately after of 50 A/m^2. For the rest of the experiments the gas production increased at the same rate than the current density applied increased. For instance, we doubled the current density applied from 150 A/m^2 to 300 A/m^2 and the gas production doubled. That was observable in every experiment except from 25 A/m^2 to 50 A/m^2. The gas production in the experiment of 50 A/m^2 was almost the triple of the one observed for the experiment with the current density of 25 A/m^2, despite only having double the current density.

This lower than expected gas production in the 25 A/m^2 is the main cause for having the best energy consumption value with the 50 A/m^2 experiment. The gas production was lower than expected due to a larger leakage in the system. Leakage occurred in all the experiments; however, it was more noticeable with experiments that used lower influent flow rates that lead to longer residence times.

As it can be seen in Figure 18, all the experiments made with a current density below 150 A/m^2 had lower energy consumptions. So, it is possible to affirm that the current density applied is a decisive parameter to reduce the systems energy consumption. Overpotential grows exponentially with the increase in the current density applied, so lower current densities will have better performances in terms of reducing the energy consumption. The lowest energy consumption obtained was 360 kJ/mol, when using a 50 A/m^2 current density, with a recovery of 34% of NaOH.

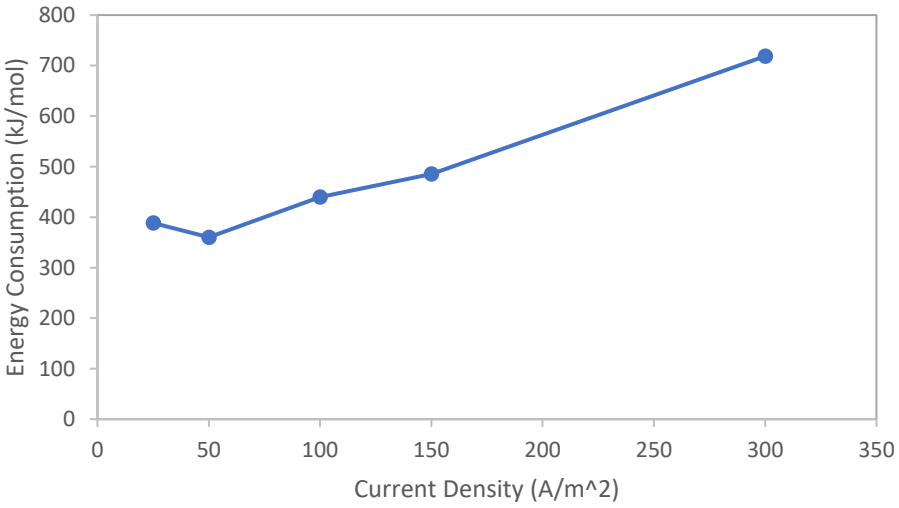

FIGURE 18 - VARIATION OF ENERGY PRODUCTION WITH INCREASING CURRENT DENSITY

5.3 Experiments with Different Sodium Concentrations

The next set of experiments was done with the fixed ideal Load Ratio of 0.8, and a Current Density of 150 A/m^2 which is not the optimal one, however allows for the system to operate faster. These experiments are described in Table 3. With these two parameters fixed, the Na^+ concentration was changed, and the flow rate was calculated taking into consideration these variables.

TABLE 3 - SET OF CONDITIONS FOR EXPERIMENTS WITH DIFFERENT SODIUM CONCENTRATIONS

Flow Rate (mL/min)	Na Concentration (mol/L)	Current Density (A/m^2)	Load Ratio
4.66	0.25	150	0.80
2.33	0.5	150	0.80
1.55	0.75	150	0.80
1.17	1.0	150	0.80
0.93	1.25	150	0.80
0.87	1.5	150	0.80

The pH shows an increase in both compartments with increasing Na^+ concentration, these changes can be seen in Figure 19. The increase is more observable in the acidifying compartment where at a concentration of 0.25M of Sodium the pH has a value of 6.12, while at a concentration of 1.5M of Sodium the pH has a value of 7.19. With a higher concentration of sodium, the flow rate we apply is lower, so the quantity of fresh ions in the solution we pump per unit of time should be the same. However, by changing the sodium concentration, we also change the equilibrium of the post capture solution, leading to an increase in the starting pH. Moreover, with a higher concentration of sodium a larger quantity of ions is introduced in the solution per unit of time. Both factors lead to this increase in pH.

Although this increase is observable, and it affects the system, it is much smaller compared to the variation observed with changing Load Ratio, which can let us confirm that the Load Ratio is the most important parameter to define the steady state pH of the system.

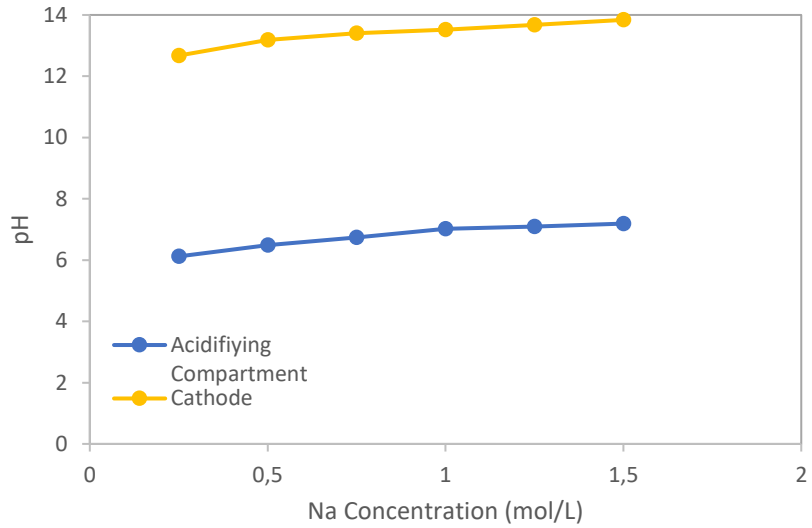

FIGURE 19 - VARIATION OF PH IN ACIDIFYING AND CATHODE COMPARTMENTS WITH INCREASING SODIUM CONCENTRATION

The CO_2 production rate has a peak at 0.5M Sodium concentration, as it can be seen in Figure 20. The higher concentrations lead to a higher pH value at steady state, and as it can be observed in Figure 8, gaseous CO_2 is produced at lower pH values, so at a higher concentration the pH is higher as explained above, and a smaller amount of carbonate and bicarbonate is transformed into carbonic acid and sequentially into CO_2.

The increase in pH leads to a gradual decline in CO_2 production, this was observable with concentrations above 0.5M. However, the experiment with 0.25M sodium concentration also presented lower CO_2 production rates than the experiment with 0.5M sodium concentration, and also lower than some experiments with even higher concentrations. Despite having a lower pH at steady state than the rest of

the experiments, when using a concentration of 0.25M we are also having a lower amount of total carbon present in the solution. This limits the amount of CO_2 that can be desorbed.

The higher concentration experiments have more carbon to be desorbed but also have higher pH values that limit the desorption capacity in the system. The balance between a low pH and having a high enough amount of carbon present in the feed solution is key to finding the ideal Na^+ concentration.

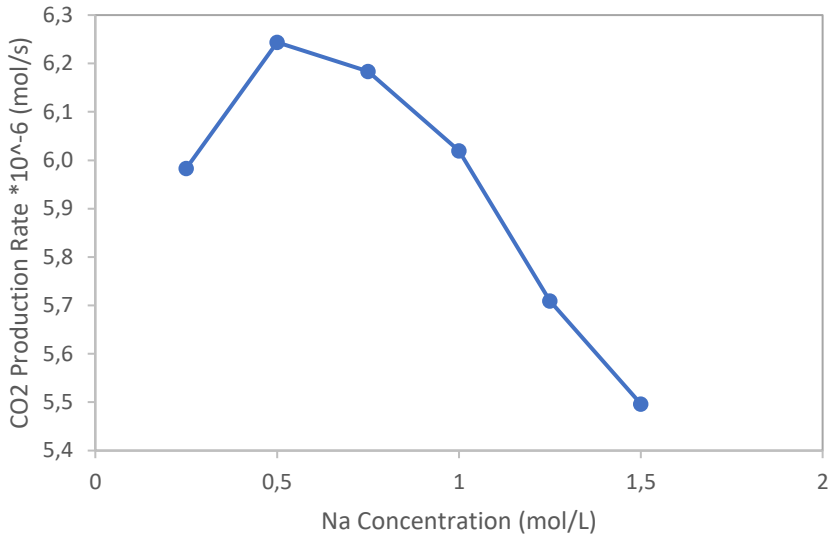

FIGURE 20 - VARIATION OF CO2 PRODUCTION RATE WITH INCREASING SODIUM CONCENTRATION

Conductivity experiences a large increase, in both compartments, with increasing sodium concentrations, as seen in Figure 21. Despite lowering the flow rates for the experiments with higher sodium concentrations to maintain the amount of Na^+ ions constant for unit of time, the initial conductivity for the post capture solution increases along with the increasing sodium concentrations.

Per unit of time we introduce the same number of ions. However, for a given moment, the higher concentrations will have more ions in a set volume inside the system. So, in this set volume there will be more ions to be moved by the current applied. And the current applied is able to move a certain amount of sodium ions, defined by the Load Ratio, in this case 80% of the sodium ions in the acidifying compartment. So, if we move the same percentage of sodium ions, the solution that has more of them per unit of volume will have more ions being transferred to the Cathode, that will react with the hydroxide and lead to a significant increase in this compartments conductivity.

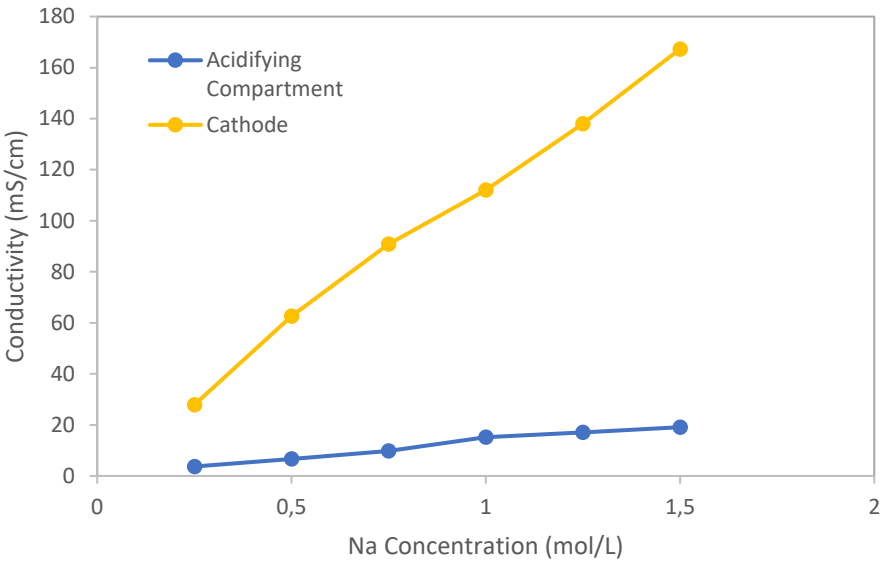

FIGURE 21 - VARIATION OF CONDUCTIVITY IN ACIDIFYING AND CATHODE COMPARTMENTS WITH INCREASING SODIUM CONCENTRATION

The lowest energy consumption observed with the experiment of 1M Na^+ concentration, as seen in figure 22, with a value of 468 kJ/mol while recovering 49% of NaOH. Despite, having a lower CO_2 production rate than the ones observed with 0.5M and 0.75M concentrations, this decrease of energy consumption is compensated by lower voltages observed.

The lower voltages are due to the higher conductivities that the experiment with 1M Na^+ concentration presented. More ions lead to a higher conductivity, subsequentially to lower resistance, and so to lower voltages.

Concentrations higher than 1M present even lower voltages, however, due to their higher pH, the gas production is much lower, and the lower voltages are not enough to offset it. So, the ideal Na^+ concentration found was 1M.

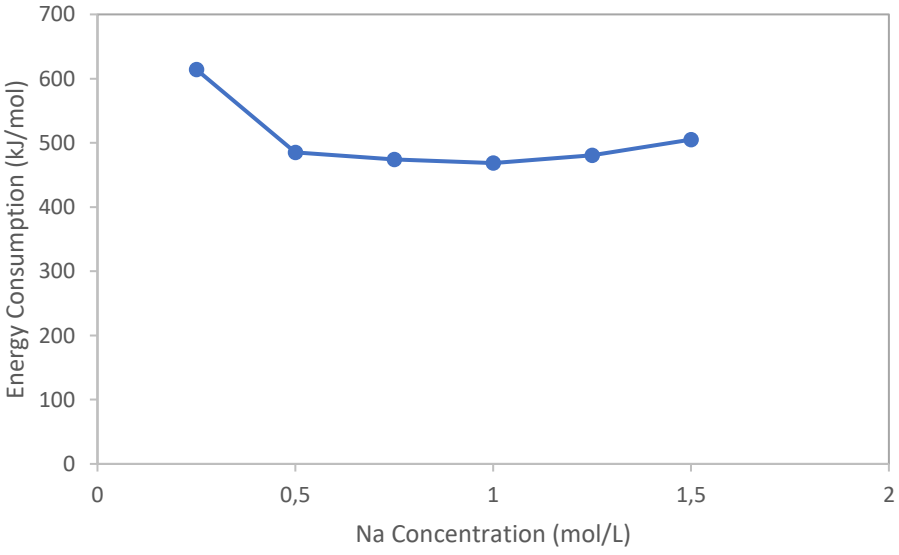

FIGURE 22 - VARIATION OF ENERGY CONSUMPTION WITH INCREASING SODIUM CONCENTRATION

5.4 Can the ideal Load Ratio be different for higher concentrations

The best energy consumption value when using a Na^+ concentration of 0.5M was obtained using a Load Ratio of 0.8. This Load Ratio proved to be the most efficient as it allowed for a good tradeoff between the CO_2 production and the voltage in the system as it did not let the conductivity drop down too much, which has seen before is problematic for the systems energy expenditure.

However, the higher concentrations present much higher conductivities as seen previously. So, these higher concentration solutions might be able to be more efficient with a higher Load Ratio, that allows for a bigger gas production, while the conductivity does not drop to a value that leads to a voltage high enough to offset the higher CO_2 production.

To assess the effects of a higher than 0.8 Load Ratio on solutions with a sodium concentration higher than 0.5M the experiments seen in Table 4 were made. The Load Ratio was set at 0.9 as a value of 1 showed an energy consumption more than three times higher for a 0.5M sodium concentration. Current was set at 150 A/m^2 to be able to run the system faster, and to be able to compare these experiments to the one made with 0.9 Load Ratio and 0.5M sodium concentration. Concentrations of 1M and 1.25M were chosen, as the former is the most energy efficient concentration observed in the previous experiments and the latter will allow us to determine a trendline related to it.

TABLE 4 - SET OF CONDITIONS FOR EXPERIMENTS WITH DIFFERENT SODIUM CONCENTRATIONS FOR A 0.9 LOAD RATIO

Flow Rate (mL/min)	Na Concentration (mol/L)	Current Density (A/m^2)	Load Ratio
1.04	1	150	0.,90
0.83	1.25	150	0.90

The trendlines observed for the pH variation with increasing concentrations for different Load Ratios can be seen in Figures 23A and 23B. The behavior of the trendline for pH is very similar in both cases. So, we can assume that changing the Load Ratio will not affect the trendlines observed if the rest of the conditions are the same.

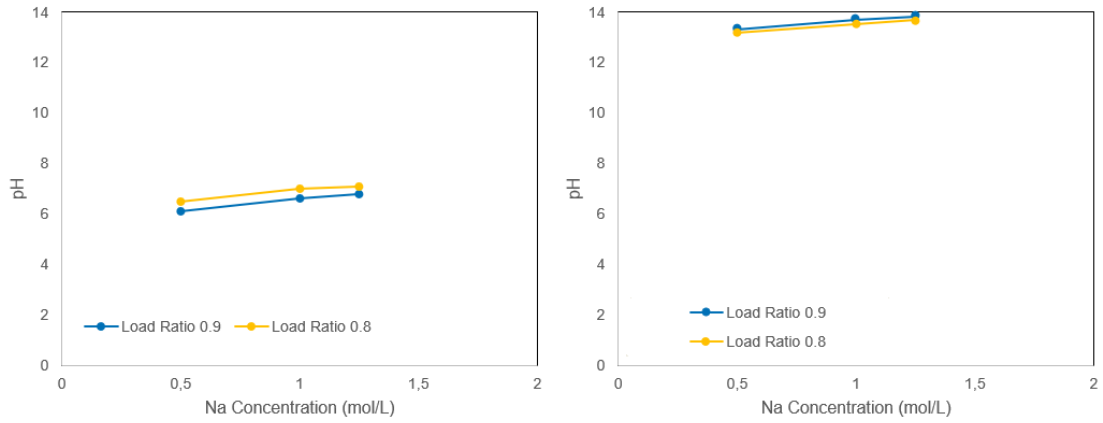

FIGURE 23 - VARIATION OF PH FOR LOAD RATIO 0.8 AND 0.9 WITH INCREASING SODIUM CONCENTRATION IN (A) ACIDIFYING COMPARTMENT AND (B) CATHODE COMPARTMENT

Conductivity also showed the same increase with increasing sodium concentration for both Load Ratios that are being compared, as seen in Figures 24A and 24B. Though it is noticeable that with increasing Na^+ concentration there is a bigger difference in conductivity between Load Ratio 0.8 and 0.9, with the latter showing lower values in the Acidifying Compartment which was expected. With a higher Load Ratio, we

are moving a higher percentage of the ions we are introducing and also desorbing more carbon, as explained previously. If we increase the concentration we have more ions present in the solution that will increase the conductivity, and so with a lower Load Ratio the increase in conductivity is larger if we increase the concentration.

The Cathode Compartment shows the same behavior although with the Load Ratio 0.8, showing lower values of conductivity, which was also expected due to the reasons stated previously.

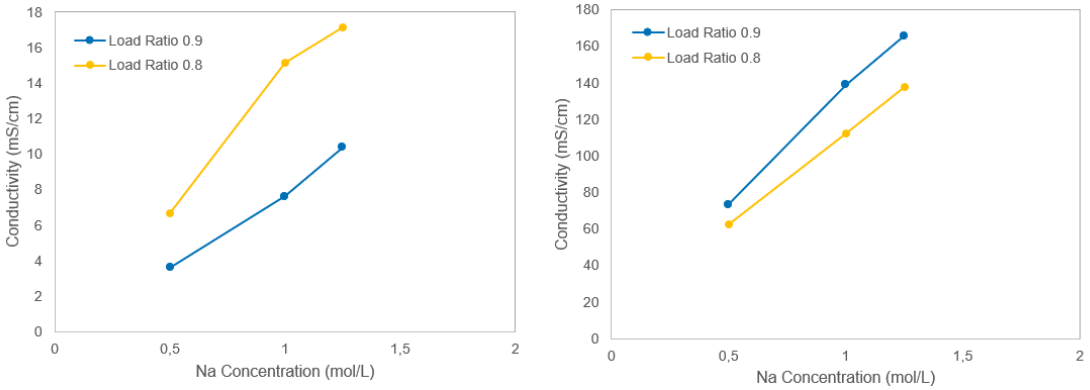

FIGURE 24 - VARIATION OF CONDUCTIVITY FOR LOAD RATIO 0.8 AND 0.9 WITH INCREASING SODIUM CONCENTRATION IN (A) ACIDIFYING COMPARTMENT AND (B) CATHODE COMPARTMENT

The CO_2 production rate follows the same pattern as it can be observed in Figure 25. For both Load Ratios the trendlines are similar with a peak at 0.5M and decreasing with an increase in Na^+ concentration.

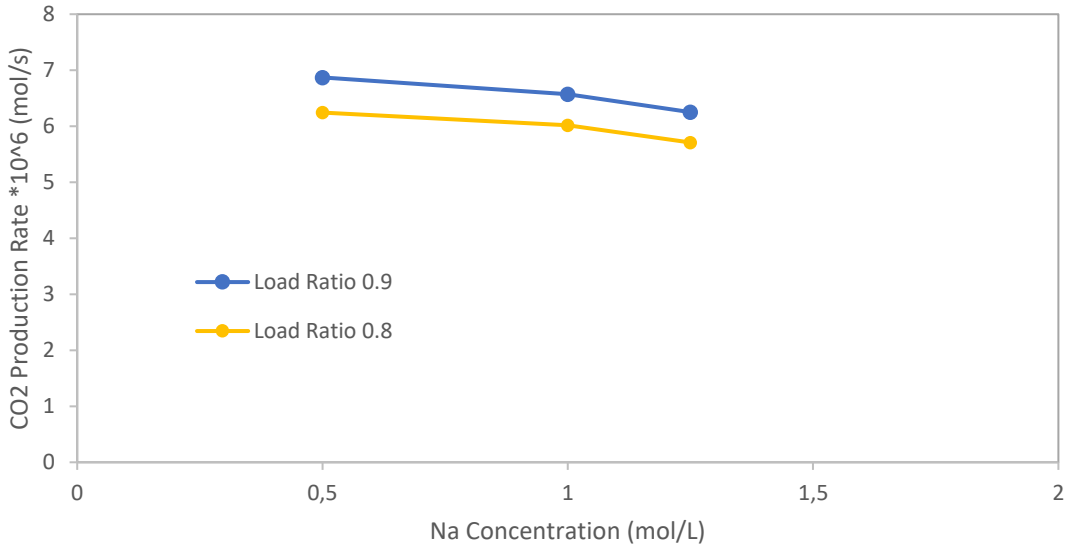

FIGURE 25 - VARIATION OF CO_2 PRODUCTION RATE FOR LOAD RATIO 0.8 AND 0.9 WITH INCREASING SODIUM CONCENTRATION

With the data these figures provide, we can assume that the trendlines for energy consumption will also follow the same pattern, and Figure 26 confirms this, with the lowest recorded energy consumption at a sodium concentration of 1M for both Load Ratios. showing that for a Load Ratio 0.9 this concentration is also the most energy efficient. However, the initial goal of this question was to find if for different concentrations the most efficient Load Ratio could be different. As it is possible to see in Figure 26 that is not the case, as the experiments done with Load Ratio 0.8 showed better results compared to 0.9 for all of the different Na^+ concentrations used.

For the concentration of 0.5M of Na^+ the energy consumption increased in 50 kJ/mol, while for the 1.25M of Na^+ concentration the increase was only of 4 kJ/mol. We can observe in Figure 26 that with increasing sodium concentrations the energy consumption difference between 0.8 and 0.9 Load Ratio gets smaller, almost reaching the same level. However, the lowest observed value is still at 0.8 Load Ratio for a concentration of 1M of Na^+.

Even though the best result was with Load Ratio 0.8 and 1M of Na^+ concentration, this lower difference in energy consumption between Load Ratio 0.8 and 0.9 that was observed for higher concentrations can mean that for concentrations higher than 1.25M of Na^+ the ideal Load Ratio may be 0.9. Further testing is required to prove this assumption. However, the fact that the difference was lower and the theoretical knowledge that by increasing the amount of ions we have in the system we can move more of them without decreasing the conductivity too much, allows us to theorize that this would be possible.

Nonetheless, this increase in sodium concentration and the use of a higher Load Ratio still should not offer a better result in terms of energy consumption as we can observe from the values obtained that the system is optimized in these two parameters.

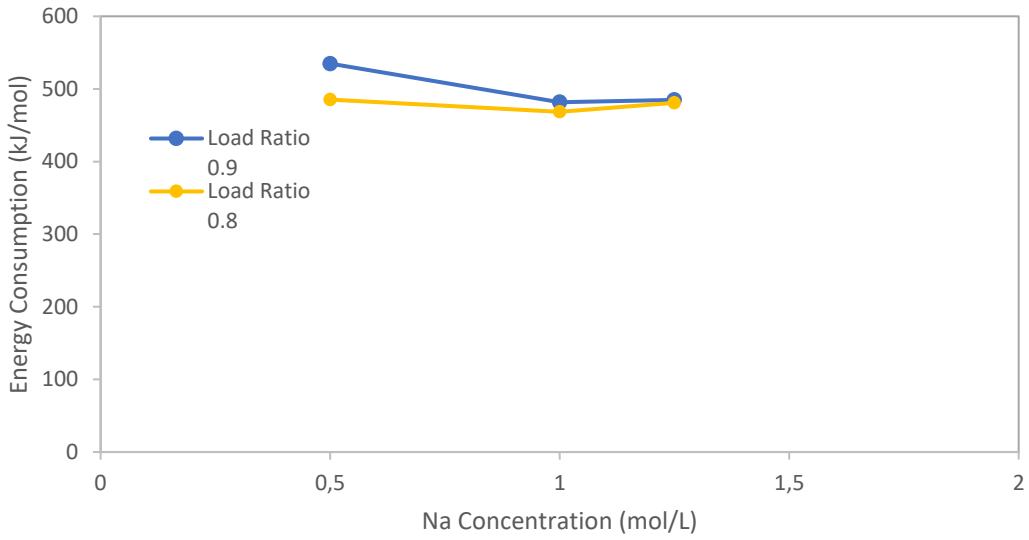

FIGURE 26 - VARIATION OF ENERGY CONSUMPTION FOR LOAD RATIO OF 0.9 AND 0.8 WITH INCREASING SODIUM CONCENTRATION

5.5 Comparing the Load Ratio influence on different Na^+ Concentrations

The last set of experiments showed that with increasing sodium concentrations different Load Ratios showed similar trendlines. Because of this, we then sought out to find if different sodium concentrations show the same trendlines for increasing Load Ratios. As it can be seen in Table 5 a new set of experiments was done for a concentration of 1M of sodium. Different Load Ratios were applied, with a fixed current density of 150 A/m^2, with a corresponding flow rate.

TABLE 5 - SET OF EXPERIMENTS WITH DIFFERENT LOAD RATIOS FOR A SODIUM CONCENTRATION OF 1M

Flow Rate (mL/min)	Na Concentration (mol/L)	Current Density (A/m^2)	Load Ratio
1.55	1	150	0.60
1.33	1	150	0.70
1.17	1	150	0.80
1.04	1	150	0.90
0.93	1	150	1

The pH variation can be seen in Figure 27. The trendlines for both concentrations are similar and the values for each Load Ratio are as well, although with two noticeable exceptions. In the Acidifying Compartment the highest Load Ratio used, which was 1, showed a bigger drop for the sodium concentration of 0.5M, in comparison with the sodium concentration of 1.0M. So, we can see that increasing the Load Ratio will have a smaller impact in the composition of the solution in the Acidifying Compartment when we use a higher Na^+ concentration. The other noticeable exception is for the lowest Load Ratio used, 0.6, in the Cathode Compartment, as the concentration of 0.5M is below the concentration of 1M by a larger margin. This is due to the Load Ratio in use desorbing less carbon so the hydroxide that we have in the Cathode ends up reacting into carbonate. With a higher concentration, the total amount of ions is large enough that even though we also have this problem of having the less conductive carbonate instead of hydroxide, the sheer amount of carbonate leads to a higher conductivity when compared to the same Load Ratio at a lower concentration.

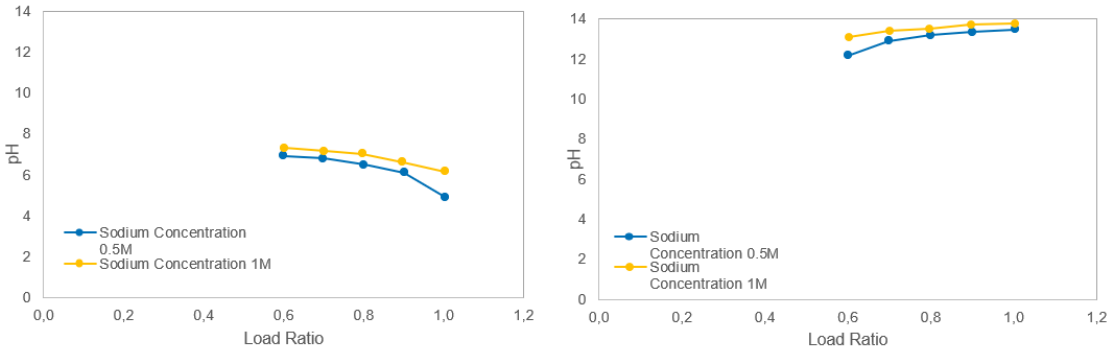

FIGURE 27 - VARIATION OF PH FOR SODIUM CONCENTRATIONS OF 0.5M AND 1M WITH INCREASING LOAD RATIO IN (A) ACIDIFYING COMPARTMENT AND (B) CATHODE COMPARTMENT

The conductivity changes in both compartments can be seen in Figure 28. The trendlines are again similar and we can verify that for a lower Load Ratio, we have a larger difference in the Acidifying Compartment for both concentrations. If we move close to 100% of the ions, the remaining solutions will have a closer conductivity than if we move 60% of the ions present. In the Cathode Compartment, if we move more ions, the difference grows larger, as we have a larger quantity of carbon being desorbed and there is more total hydroxide that increases significantly the conductivity.

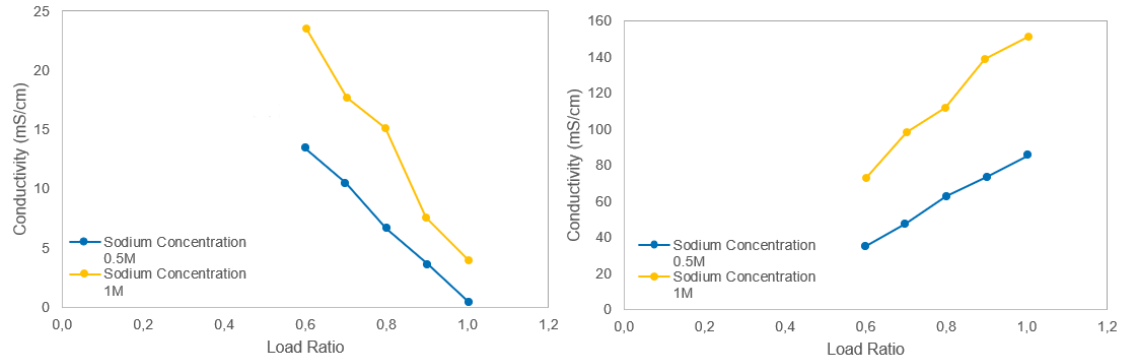

FIGURE 28 - VARIATION OF CONDUCTIVITY FOR SODIUM CONCENTRATION OF 0.5M AND 1M WITH INCREASING LOAD RATIO IN (A) ACIDIFYING COMPARTMENT AND (B) CATHODE COMPARTMENT

As it is seen in Figure 27, the pH in the Acidifying Compartment is higher with a higher concentration, and the gap grows larger with increasing Load Ratio. This explains what is seen in Figure 29. Initially the higher concentration shows a bigger CO_2 production rate, due to having more total carbon species to be desorbed. However, when we increase the Load Ratio, the pH decreases more in the lower concentration

solution. With a lower pH we can desorb more carbon as seen previously, so we end up having a higher CO_2 production rate when using a lower concentration, for a Load Ratio higher than 0.8.

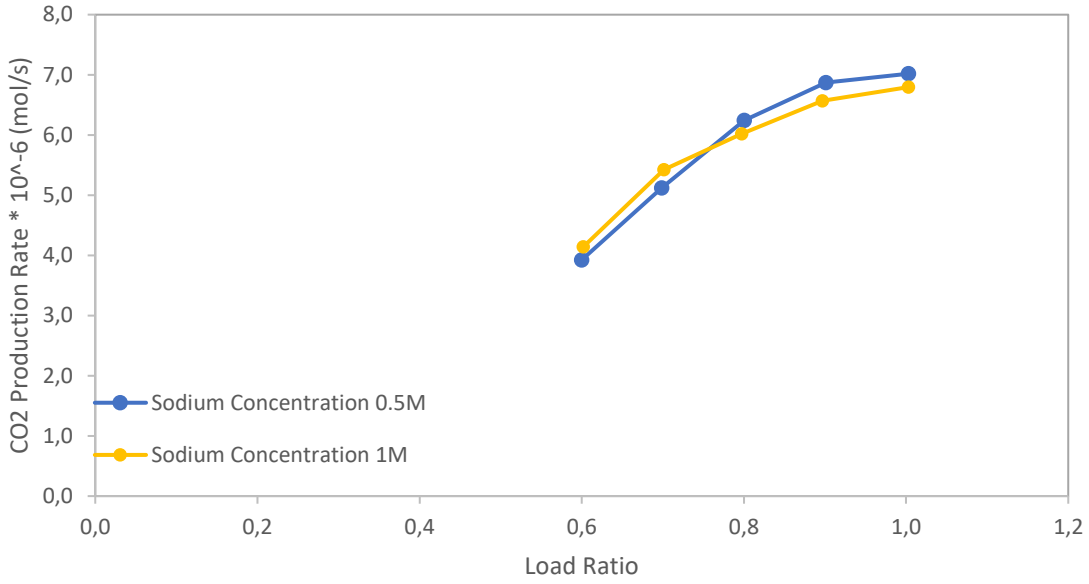

FIGURE 29 - VARIATION OF CO_2 PRODUCTION RATE FOR SODIUM CONCENTRATION OF 0.5M AND 1M WITH INCREASING LOAD RATIO

The energy consumption also shows a similar trendline, with one exception, as it can be observed in Figure 30. For Load Ratios lower than 1, both trendlines are very similar, with the values being close as well. However, for Load Ratio 1, the concentration of 0.5M as a spike and more than doubles the energy consumption for Load Ratio 0.8. While for a concentration of 1M, the energy consumption only slightly increases. This can be explained by the conductivities observed in the Acidifying Compartment. Although the difference got smaller when increasing the Load Ratio, all the values for conductivity in this compartment were still above 3mS/cm, except the value for the concentration of 0.5M with a Load Ratio of 1, as this value was below 1mS/cm. So, despite showing a smaller difference for the experiment with a corresponding Load Ratio and higher concentration in comparison with remaining experiments, this less than 1mS/cm value is low enough that the energy consumption increases considerably.

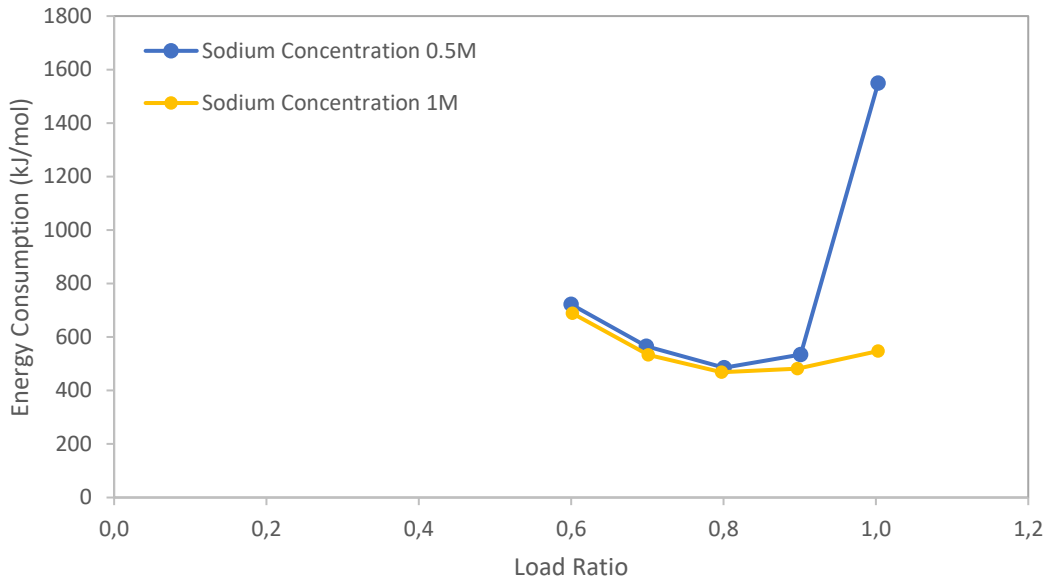

FIGURE 30 - VARIATION OF ENERGY CONSUMPTION FOR SODIUM CONCENTRATION OF 0.5M AND 1M WITH INCREASING LOAD RATIO

6 CONCLUSIONS

The experiments made showed that the Load Ratio is the parameter that influences the system the most, with the best results being obtained at a Load Ratio of 0.8. The system was the most efficient with a Current Density of 50 A/m^2 and a Na^+ concentration of 1M. The best energy consumption result obtained was 360 kJ/mol. However, this value can still be lowered as it was obtained using a Na^+ concentration of 0.5M. Due to time constrictions an experiment that combined the optimized parameters for Load Ratio, Current Density and sodium concentration was not done, still, with what we learned from the remaining experiments it is possible to conclude that the energy consumption would be lower if we used them.

The value of 360 kJ/mol equals 8.18 GJ/ton, which is lower than the 8.81 GJ/ton that Carbon Engineering reports when using natural gas to fuel their process. This shows that the system studied in this work can be competitive and presents itself as an alternative to CO_2 desorption processes in use.

Further research is still needed as the system can be improved. The use of a material for the Cathode more adequate to the reactions observed there would decrease the overpotential losses and reduce the energy consumption of the system. The upscaling of the system can also be of importance for future studies as it will lead to a larger quantity of CO_2 being desorbed by the system, but it also might be able to reduce the energy consumption of the system. The upscaling should be done in two fronts, by augmenting the membrane area, and by adding more cell pairs. A larger membrane area implies a new system as the housing of the current system as well as the electrodes are designed for a 100 cm^2 membrane. The addition of more cell pairs requires additional studying as it would need to use bipolar membranes, which were not used in this work and would need a complete overhaul of the setup.

The solution extracted out of the Cathode Compartment can be used in the future to capture more atmospheric CO_2. This solution is composed by NaOH and by sodium carbonate and bicarbonate, with the composition changing depending on the conditions of the experiment. So, in the future a recirculation mechanism can be added to the system to desorb the remaining carbonate and bicarbonate. Using the resulting solution to capture more CO_2 is also feasible and for future applications it might be interesting to use conditions that do not give the best energy consumption results but in which the composition of the solution extracted from the Cathode Compartment has a higher percentage of NaOH. It also might be interesting for certain applications to use a higher Current Density than the optimal one to improve the speed of the process and therefore the amount of total carbon that the system can desorb. These are considerations that can be further studied for practical applications in a larger scale. However, at lab scale the system showed the versatility to handle all these changing parameters and still be competitive in energy consumption.

It should be noted that despite DAC being a necessary tool to prevent climate change it should not be the only tool for it, as a reduction in emissions and the preservation of natural habitats and forests is still necessary to maintain the biosphere.

7 REFERENCES

Aggarwal, P., & Singh, A. (2010). Implications of global climatic change on water and food security. In *Global Change: Impacts on water and food security* (pp. 49-63): Springer.

Alesi Jr, W. R., & Kitchin, J. R. (2012). Evaluation of a primary amine-functionalized ion-exchange resin for CO2 capture. *Industrial & Engineering Chemistry Research, 51*(19), 6907-6915.

Allen, M., Dube, O., Solecki, W., Aragón-Durand, F., Cramer, W., Humphreys, S., Kainuma, M., Kala, J., Mahowald, N., & Mulugetta, Y. (2018). Framing and context. *Global Warming of, 1*, 49-91.

Archer, D., & Brovkin, V. (2008). The millennial atmospheric lifetime of anthropogenic CO2. *Climatic Change, 90*(3), 283-297.

Baciocchi, R., Storti, G., & Mazzotti, M. (2006). Process design and energy requirements for the capture of carbon dioxide from air. *Chemical Engineering and Processing: Process Intensification, 45*(12), 1047-1058.

Broehm, M., Strefler, J., & Bauer, N. (2015). Techno-economic review of direct air capture systems for large scale mitigation of atmospheric CO2. *Available at SSRN 2665702*.

Cheung, O., & Hedin, N. (2014). Zeolites and related sorbents with narrow pores for CO 2 separation from flue gas. *Rsc Advances, 4*(28), 14480-14494.

Ciais, P., Sabine, C., Bala, G., Bopp, L., Brovkin, V., Canadell, J., Chhabra, A., DeFries, R., Galloway, J., & Heimann, M. (2014). Carbon and other biogeochemical cycles. In *Climate change 2013: the physical science basis. Contribution of Working Group I to the Fifth Assessment Report of the Intergovernmental Panel on Climate Change* (pp. 465-570): Cambridge University Press.

Fasihi, M., Efimova, O., & Breyer, C. (2019). Techno-economic assessment of CO2 direct air capture plants. *Journal of cleaner production, 224*, 957-980.

Field, C. B., Barros, V., Stocker, T. F., & Dahe, Q. (2012). *Managing the risks of extreme events and disasters to advance climate change adaptation: special report of the intergovernmental panel on climate change*: Cambridge University Press.

Goeppert, A., Czaun, M., Prakash, G. S., & Olah, G. A. (2012). Air as the renewable carbon source of the future: an overview of CO 2 capture from the atmosphere. *Energy & Environmental Science, 5*(7), 7833-7853.

Hart, M. H. (1978). The evolution of the atmosphere of the Earth. *Icarus, 33*(1), 23-39.

Hartmann, D. L., Tank, A. M. K., Rusticucci, M., Alexander, L. V., Brönnimann, S., Charabi, Y. A. R., Dentener, F. J., Dlugokencky, E. J., Easterling, D. R., & Kaplan, A. (2013). Observations: atmosphere and surface. In *Climate change 2013 the physical science basis: Working group I contribution to the fifth assessment report of the intergovernmental panel on climate change* (pp. 159-254): Cambridge University Press.

Hayashi, H., Taniuchi, J., Furuyashiki, N., Sugiyama, S., Hirano, S., Shigemoto, N., & Nonaka, T. (1998). Efficient recovery of carbon dioxide from flue gases of coal-fired power plants by cyclic fixed-bed operations over K2CO3-on-carbon. *Industrial & Engineering Chemistry Research, 37*(1), 185-191.

House, K. Z., Baclig, A. C., Ranjan, M., van Nierop, E. A., Wilcox, J., & Herzog, H. J. (2011). Economic and energetic analysis of capturing CO2 from ambient air. *Proceedings of the National Academy of Sciences, 108*(51), 20428-20433.

Karl, T. R., & Trenberth, K. E. (2003). Modern global climate change. *science, 302*(5651), 1719-1723.

Keith, D. W., Holmes, G., St. Angelo, D., & Heidel, K. (2018). A Process for Capturing CO2 from the Atmosphere. *Joule, 2*(8), 1573-1594.

Kuntke, P., Rodriguez Arredondo, M., Widyakristi, L., Ter Heijne, A., Sleutels, T. H., Hamelers, H. V., & Buisman, C. J. (2017). Hydrogen Gas Recycling for Energy Efficient Ammonia Recovery in Electrochemical Systems. *Environmental Science and Technology, 51*(5), 3110-3116.

Lackner, K., Ziock, H.-J., & Grimes, P. (1999). *Carbon dioxide extraction from air: is it an option?*

Leeson, D., Mac Dowell, N., Shah, N., Petit, C., & Fennell, P. S. (2017). A Techno-economic analysis and systematic review of carbon capture and storage (CCS) applied to the iron and steel, cement, oil refining and pulp and paper industries, as well as other high purity sources. *International Journal of Greenhouse Gas Control, 61*, 71-84.

MacDowell, N., Florin, N., Buchard, A., Hallett, J., Galindo, A., Jackson, G., Adjiman, C. S., Williams, C. K., Shah, N., & Fennell, P. (2010). An overview of CO2 capture technologies. *Energy & Environmental Science, 3*(11), 1645-1669.

Matthews, H. D., & Caldeira, K. (2008). Stabilizing climate requires near-zero emissions. *Geophysical Research Letters, 35*(4).

Nagasawa, H., Yamasaki, A., Iizuka, A., Kumagai, K., & Yanagisawa, Y. (2009). A new recovery process of carbon dioxide from alkaline carbonate solution via electrodialysis. *AIChE Journal, 55*(12), 3286-3293.

Newman, J., & Thomas-Alyea, K. E. (2012). *Electrochemical systems*: John Wiley & Sons.

Oschatz, M., & Antonietti, M. (2018). A search for selectivity to enable CO 2 capture with porous adsorbents. *Energy & Environmental Science, 11*(1), 57-70.

Ping, E., Sakwa-Novak, M., & Eisenberger, P. (2018). *Global thermostat low cost direct air capture technology.* Paper presented at the International Conference on Negative CO2 Emissions, Gothenburg, May.

Plaza, M., García, S., Rubiera, F., Pis, J., & Pevida, C. (2010). Post-combustion CO2 capture with a commercial activated carbon: comparison of different regeneration strategies. *Chemical Engineering Journal, 163*(1-2), 41-47.

Radosz, M., Hu, X., Krutkramelis, K., & Shen, Y. (2008). Flue-gas carbon capture on carbonaceous sorbents: toward a low-cost multifunctional carbon filter for “green” energy producers. *Industrial & Engineering Chemistry Research, 47*(10), 3783-3794.

Rodriguez Arredondo, M., Kuntke, P., Ter Heijne, A., Hamelers, H. V. M., & Buisman, C. J. N. (2017). Load ratio determines the ammonia recovery and energy input of an electrochemical system. *Water Res, 111*, 330-337.

Ruddiman, W. F. (2003). The anthropogenic greenhouse era began thousands of years ago. *Climatic Change, 61*(3), 261-293.

Sanz-Perez, E. S., Murdock, C. R., Didas, S. A., & Jones, C. W. (2016). Direct capture of CO2 from ambient air. *Chemical Reviews, 116*(19), 11840-11876.

Vogel, A. (2017). CO2 - the Raw Material that Comes from AIR. *Swiss Federal Office of Energy*.

Willauer, H. D., DiMascio, F., Hardy, D. R., Lewis, M. K., & Williams, F. W. (2011). Development of an Electrochemical Acidification Cell for the Recovery of CO2and H2from Seawater. *Industrial & Engineering Chemistry Research, 50*(17), 9876-9882.

Winton, D., Isobe, J., Henson, P., MacKnight, A., Yates, S., & Schuck, D. (2016). *Carbon Dioxide Removal Technologies for Space Vehicles-Past, Present, and Future*.

Yu, C.-H., Huang, C.-H., & Tan, C.-S. (2012). A review of CO2 capture by absorption and adsorption. *Aerosol Air Qual. Res, 12*(5), 745-769.